

AD A094963

LEVEL II

(12)
B.S.

**SECOND
TECHNICAL PROGRESS REPORT**

of

CONTRACT N00014-75-0469
(M.I.T. OSP #82558)

**STUDY OF
RESIDUAL STRESSES AND DISTORTION IN
STRUCTURAL WELDMENTS
IN HIGH-STRENGTH STEELS**

by

VASSILIOS J. PAPAZOGLOU
AND
KOICHI MASUBUCHI

to

OFFICE OF NAVAL RESEARCH

NOVEMBER 30, 1980

DTIC
ELECTE
S FEB 20 1981 D

E

DOC. FILE COPY

DISTRIBUTION STATEMENT A
Approved for public release;
Distribution Unlimited

MASSACHUSETTS INSTITUTE OF TECHNOLOGY
CAMBRIDGE, MASSACHUSETTS

81 2 19 04

MASSACHUSETTS INSTITUTE OF TECHNOLOGY
DEPARTMENT OF OCEAN ENGINEERING ✓
CAMBRIDGE, MASS. 02139

9 SECOND
TECHNICAL PROGRESS REPORT. no. 2,

15 of
Contract N00014-75-C-0469
(MIT OSP #82558)

6 STUDY OF RESIDUAL STRESSES AND DISTORTION
IN STRUCTURAL WELDMENTS IN HIGH-STRENGTH STEELS.

to

Office of Naval Research

11 32 Nov 1980

12 73

by

10 Vassilios J. Papazoglou
Koichi Masubuchi

40-856
~~220~~

REPORT DOCUMENTATION PAGE		READ INSTRUCTIONS BEFORE COMPLETING FORM
1. REPORT NUMBER Technical Progress Report	2. GOVT ACCESSION NO. AD-A094963	3. RECIPIENT'S CATALOG NUMBER
4. TITLE (and Subtitle) STUDY OF RESIDUAL STRESSES AND DISTORTION IN STRUCTURAL WELDMENTS IN HIGH-STRENGTH STEELS		5. TYPE OF REPORT & PERIOD COVERED
		6. PERFORMING ORG. REPORT NUMBER
7. AUTHOR(s) Vassilios J. Papazoglou and Koichi Masubuchi		8. CONTRACT OR GRANT NUMBER(s) Contract N00014-75-0469 (M.I.T. OSP #82558)
9. PERFORMING ORGANIZATION NAME AND ADDRESS Massachusetts Institute of Technology 77 Massachusetts Avenue, Cambridge MA 02139		10. PROGRAM ELEMENT, PROJECT, TASK AREA & WORK UNIT NUMBERS
11. CONTROLLING OFFICE NAME AND ADDRESS Department of the Navy Office of Naval Research Arlington, Virginia 22217		12. REPORT DATE November 30, 1980
		13. NUMBER OF PAGES
14. MONITORING AGENCY NAME & ADDRESS (if different from Controlling Office)		15. SECURITY CLASS. (of this report) Unclassified
		15a. DECLASSIFICATION/DOWNGRADING SCHEDULE
16. DISTRIBUTION STATEMENT (of this Report) This document has been approved for public release and sale; its distribution is unlimited. Reproduction in whole or in part is permitted by the U.S. Government.		
17. DISTRIBUTION STATEMENT (of the abstract entered in Block 20, if different from Report)		
18. SUPPLEMENTARY NOTES		
19. KEY WORDS (Continue on reverse side if necessary and identify by block number) Welding Residual Stresses Distortion High Strength Steels		
20. ABSTRACT (Continue on reverse side if necessary and identify by block number) Experimental results on temperature, strain and distortion during welding HY-130 steel are presented. The geometries include 1 inch thick plates and 0.75 inch cylindrical shells. Welding was performed using the gas metal arc, electron beam and laser processes. The experimental results are compared with predictions made by computer programs. Finally, through thickness distributions of residual stresses obtained using the Rosenthal-Norton sectioning technique are presented.		

EXECUTIVE SUMMARY

This report presents the progress made during the third year of the O.N.R. sponsored research program entitled "Study of Residual Stresses and Distortion in Structural Weldments in High-Strength Steels", and consists of two tasks.

Regarding the first task which deals with thick plates a substantial amount of experiments were performed measuring temperatures, transient strains and distortion during welding various HY-130 steel specimens. The Electron Beam (EB) and Gas Metal Arc (GMA) welding processes were used on simply supported, simple restrained (H-type groove) and restrained cracking test (window test) specimens. A total of fourteen (14) specimens were welded, some of which were made of SAE 1020 mild steel for comparison purposes. The report presents results of the measurements taken, as well as comparisons with analytical predictions.

The triaxial distribution of residual stresses was also measured at a few locations of three of the above specimens - one EB and two GMA welded - using the Rosenthal-Norton sectioning technique. Comparisons of the obtained results among themselves as well as with other available data were performed. Finally, the strain energy release rate was obtained indirectly, through crack opening displacement measurements, for the simple restrained specimens.

On the analytical side, a finite element linear elastic computer program was developed capable of calculating the joint degree of constraint for any flat geometry. Heat transfer analyses were also performed using newly developed analytical solutions based on a finite heat source model as well as using the multipurpose nonlinear heat transfer finite element computer program ADINAT which was modified to take into account latent heat effects. Finally, modifications were made on the thermal-elastic-plastic finite element program ADINA by incorporating the effect of phase transformations.

Regarding the second task, which deals with cylindrical shells, the residual stresses were measured - using electric resistance strain gages and the strain relaxation technique - on the girth-welded cylinder prepared during the second year of this research effort. The axial and tangential residual stresses, as distributed in both the axial and circumferential directions, were determined and compared with data from other investigators.

All in all, therefore, the proposed program of research was carried out as originally proposed. A final report is expected to be issued at the conclusion of the four-year study.

Access of Copy	
NWIS Serial	<input checked="" type="checkbox"/>
DTIC TAB	<input type="checkbox"/>
Unannounced	<input type="checkbox"/>
Justification	
By _____	
Distribution/	
Availability Codes	
Dist	Avail and/or Special
A	

TABLE OF CONTENTS

	PAGE
1. Introduction	1
2. Progress of Task 1 - Thick Plates.	6
2.1 General Status.	6
2.2 Development of Details of the Research Plan for the Third Year (Step 1.8)	6
2.3 Measurement of Residual Stress in Butt-Welded Thick Plates (Step 1.5)	7
2.3.1 EB Welding Tests	8
2.3.2 GMA Welding Tests.	15
2.4 Experiments on Simple Restrained Butt Welds (Step 1.6). . .	27
2.4.1 Experimental Procedure	27
2.4.2 Results.	30
2.5 Experiment on Restrained Cracking Test Specimen (Step 1.9). .	36
2.5.1 Description and Experimental Procedure	36
2.5.2 Results.	38
2.6 Measurement of Strain Energy Release on Specimens Made in 1.6 and 1.9 (Step 1.10)	40
2.7 Analysis of Data (Steps 1.7 and 1.11)	46
2.7.1 Joint Degree of Constraint	46
2.7.2 Heat Transfer Analysis	49
2.7.3 Stress Analysis.	53
3. Progress of Task 2 - Cylindrical Shells.	55
3.1 General Status.	55
3.2 Development of Details of the Research Plan (Step 2.8). . .	55
3.3 Measurement of Residual Stresses in Specimen Made in 2.6 (Step 2.10)	55
3.3.1 Experimental Procedure	55
3.2.2 Residual Stress Distributions.	56

	PAGE
4. Publications and Degrees Granted	65
4.1 Publications.	65
4.1.1 Books.	65
4.1.2 Papers	65
4.2 Degrees Granted	65
4.3 Theses Completed.	66

1. INTRODUCTION

The objective of this research program, which started on December 1, 1977, is to analytically and experimentally study residual stresses and distortion in structural weldments in high-strength steel.

This program includes (1) generation of experimental data and (2) development of analytical systems. HY-130 is the primary material to be investigated; a limited number of experiments are, however, to be conducted using low-carbon steel specimens. Experiments are to be made using the multipass gas metal arc welding and electron-beam welding (one-pass) process.

More specifically,

Materials: HY-130 steel (with some control specimens in low-carbon steel)

Thickness: 1 inch (with some specimens 1/2" thick)

Welding processes: Electron beam (EB) and multipass gas metal arc (GMA) processes

Specimen geometries: The following types of specimens are considered

- a. Butt welds in thick plates
 - (1) Unrestrained butt welds
 - (2) Simple restrained butt welds
 - (3) Restrained welds simulating practical weldments
- b. Girth welds of cylindrical shells
 - (4) Girth welding along the groove of a cylindrical shell
 - (5) Girth welding between unstiffened cylindrical shells.

The work to be performed has been divided into two main tasks:

Task 1: Research on butt welds in thick plates

Task 2: Research on girth welds in cylindrical shells

The entire program is expected to be completed in three years.

Table 1.1 illustrates the tasks and phases included in this study. The

planned progress for each task appears in the original proposal, dated July 1977.

Table 1.2 summarizes test conditions and the number of specimens to be prepared. Since the major effort of the proposed research is to develop analytical systems, experiments will be made on a few specimens to verify the analysis. Table 1.3 illustrates how analyses will be improved during the three-year program.

Three progress reports, dated October 10, 1978, August 31, 1979 and July 15, 1980 and a technical progress report, dated November 30, 1979, have already been issued. This second technical report consolidates the information contained in the third progress report and the progress made since then; it essentially covers the efforts carried out during the third year of the research program and should be considered as a companion to the first progress report.

Note that no final report of the program is issued at this time, as preplanned according to Table 1.1, because of a request for a one-year extension of the program to November 30, 1981 as per a formal proposal dated November 1980. This program extension would cover the following tasks:

Task 3: Development of information on weldments in bronze

Task 4: Research on thermal stress relieving of weldments

Task 5: Development of improved computer programs.

It is expected that a final report covering all tasks previously mentioned will be issued at the end of the program extension.

For the most part the program has been carried out as originally proposed. The few changes made as well as work in the final stages of completion will be dealt with in the appropriate places.

TABLE 1.1 Tasks and Phases of the Program

	Task 1: Thick Plate	Task 2: Cylindrical Shell
First Year	1.1 Develop details of research plan	2.1 Develop details of research plan
	1.2 Experiments on unrestrained butt welds	2.2 Experiment on girth welding along groove of a cylindrical shell
	1.3 Analysis of data obtained in 1.2	2.3 Analysis of data obtained in 2.2
Second Year	1.4 Develop details of research plan	2.4 Develop details of research plan
	1.5 Measurement of residual stresses in specimens made in 1.2	2.5 Measurement of residual stresses in specimens made in 2.2
	1.6 Experiment on simple restrained butt welds	2.6 Experiment on butt welds between unstiffened cylindrical shells
	1.7 Analyses of data obtained in 1.5 and 1.6	2.7 Analyses of data obtained in 2.5 and 2.6
Third Year	1.8 Develop details of research plan	2.8 Develop details of research plan
	1.9 Experiment on restrained cracking test specimens	2.9 ---
	1.10 Measurement of strain energy release on specimens made in 1.6 and 1.9	2.10 Measurement of residual stresses in specimens made in 2.6
	1.11 Analysis of data obtained in 1.9 and 1.10	2.11 Analysis of data obtained in 2.10
Preparation of the Final Report		

Information on residual stresses and strain energy release in specimens used for weld cracking and stress-corrosion cracking

Information on residual stresses and distortion of welded cylindrical shells

TABLE 1.2 Experimental Conditions and Number of Specimens

Year	Steps	Processes	Specimen Geom.		Total	
			Thick Plate	Cylindrical Shell		
			1" thick			1/2" thick
			Low-carbon steel	HY-130		HY-130
First Year	1.2	EB	$1 + \alpha^{(1)}$	$1 + \alpha^{(1)}$	$5(1 + \alpha)$	
	2.2	GMA	$1 + \alpha$	$1 + \alpha^{(1)}$		
Second Year	1.5	EB	Specimens made in 1.2 & 2.2 will be used			
	2.5	GMA				
	1.6	EB	-	2	-	$5 + \alpha$
	2.6	GMA	-	2	$1 + \alpha$	
Third Year	1.9	EB		$1 + \alpha^{(2)}$	$2(1 + \alpha)$	
		GMA		$1 + \alpha^{(2)}$		
	1.10	EB	Specimens made in 1.6 & 2.6 will be used			
	2.10	GMA				

NOTE: (1) $(1 + \alpha)$ means that two specimens will be prepared, of which one will be the primarily specimen. If the first test is conducted successfully, only a limited experiment will be made on the second specimen.

(2) 2-inch thick plate may be used.

TABLE 1.3 Planned Improvements of Analyses

Current Status	I.0. Manuals #3, #4, #5	II.0. Muraki's analysis
First Year	<u>Unrestrained Butt Welds</u> I.1. Modify to improve compatibility	<u>Groove Weld</u> II.1. Modify to improve compatibility
	I.2. Include effects of metallurgical transformation	II.2. Develop simple analyses
	I.3. Include analysis of multipass welding	
Second Year	I.4. Analysis of residual stress	II.3. Analysis of residual stress
	I.5. Include effects of restraint	II.4. Include effects of metallurgical transformation
	I.6. Develop analysis of strain energy release	II.5. Include analysis of multipass welding
Third Year	I.7. Develop analysis of practical restrained specimens	(II.6. Possible analysis of effect of stiffeners)
	I.8. Develop final versions of computer programs	II.7. Develop final versions of computer programs

NOTE: This table lists those activities related to improvement of analyses. Efforts which will be spent for analyzing existing data, and possible modification of programs are not included here.

2. PROGRESS OF TASK 1 - THICK PLATES
DECEMBER 1, 1979 to NOVEMBER 30, 1980

2.1 General Status

According to the original proposal, dated July, 1977, the research during the third year would include the following, under Task 1:

- 1.8 Develop details of research plan
- 1.9 Experiment on restraint cracking test specimens
- 1.10 Measurement of strain energy release made in 1.6¹ and 1.9
- 1.11 Analysis of data obtained in 1.9 and 1.10

The research program has been mostly carried out as originally proposed. Some final work is still being carried out on the analytical modelling of the welding progress.

2.2 Development of Details of the Research Plan for the Third Year(Step 1.8).

It was decided that experiments would be made to determine changes of temperatures, thermal strains, and joint transverse shrinkage in simple restrained butt welds. This task was a continuation of the one started during the second year and detailed in the first progress report. Details of the experiments are included in Section 2.4.

In addition, experiments would be carried out to measure temperatures and transient strains on the restrained cracking test specimen used by the Navy to investigate cracking susceptibility (Step 1.9).

Moreover, given the initial success of the experiments performed during the second year on 1020 EB welded specimens for measuring the triaxial distribution of residual stresses using the Rosenthal-Norton sectioning technique², it was decided that further experiments should be

¹Step 1.6 reads: "Experiments on simple restrained butt welds". It has been initiated during the second year and was completed during the first months of the third year of this research program.

²Rosenthal, D. and Norton, J.T., "A Method of Measuring Triaxial Residual Stress in Plates", Welding Journal, 24 (5), May 1954, pp. 295-s to 307-s.

performed on HY-130 specimens. Upon investigation of the already available specimens, however, it was discovered that most of them had extended amounts of undercutting, a fact that made them unsuitable for reliable residual stress measurements. As a result of this, it was decided that a new welding experiment should be performed using the EB process and trying to ensure the absence of undercutting. Details of this experiment and the subsequent measurement of residual stresses are covered in the next section. Furthermore, it was decided that new GMA welds should be made and measurements of their triaxial distribution of residual stresses undertaken so as to study the effect of multipass welding on residual stresses. Details of these experiments are also covered in the next section.

Regarding Step 1.10, the measurement of the strain energy release rate was decided to be performed indirectly through measurement of the crack opening displacement (COD) in the simply restrained specimens.

Finally, progress has also been made as far as the analytical area is concerned. A linear elastic finite element analysis has been performed for the calculation of the degree of constraint in the restrained specimens. Moreover, the phase transformation option has already been coded in the finite element heat transfer program ADINAT; initial results seem to be very encouraging. The coding of phase transformation effects in the multiple purpose finite element stress analysis program ADINA has been concluded and is currently being tested for accuracy.

2.3 Measurement of Residual Stresses in Butt-Welded Thick Plates(Step 1.5).

This section covers the continuation of Step 1.5 which has been initiated during the second year of this research program. It details the results obtained in the case of HY-130 plates.

The following theses, dealing with this step, have been completed or are near completion: Coumis, George A., "An Experimental Investigation of the Transient Thermal Strain Variation and the Triaxial Residual Stress Field Generated due to Electron Beam Welding of Thick HY-130 Plates", S.M. Thesis, M.I.T., June 1980. Sousa Sa, P.A., "Investigation of Triaxial

Residual Stress Distribution Remaining after GMA Welding of Thick HY-130 Steel Plates", O.E. Thesis, M.I.T., to be submitted on January 15, 1980.

2.3.1 EB Welding Tests.

Welding Procedure. The electron-beam welding tests were carried out by Coumis using the facilities of the Applied Energy Company, Stoneham, Mass. since no appropriate facilities were available at M.I.T. A Hamilton Zeiss Model SWS machine capable of providing a maximum power of 7.5 kW at 150 kV and 50mA was used. The welding was performed in a vacuum chamber 54 in. in diameter and 96 in. long. During the experiment the vacuum obtained measured 2×10^{-4} torr.

An extensive investigation was initially carried out to determine the appropriate welding parameters that would ensure the absence of undercutting in the final welded specimen. It should be noted that such an investigation was necessary because the previous experiments, conducted during the first year, produced specimens with undercuts, a fact that made them unsuitable for residual stress measurements on the weld line.

A total of fourteen (14) specimens were used for this investigation that searched for best values of the welding speed, voltage, amperage, workpiece distance, and beam focusing distance. The criterion used was full 1 in. penetration along the total joint length with no undercuts, and using the least possible heat input.

Based on the results obtained from the above experiments the following was decided to be the combination of parameters that would produce the best weld:

Voltage	=	150kV
Amperage	=	45mA
Welding speed	=	0.25 in/sec (15 ipm)
Workpiece distance	=	15.5 in.
Focusing distance	=	15.75 in.
Copper backing along total weld length		

Two plates 24 5/16" x 13" x 1" made of HY-130 steel were welded using the above parameters. The groove shape was square butt with a maximum of

unforced contact tolerance equal to 0.005". A copper backing strip 26" x 1/2" x 1/4" was installed along the whole joint length. Two tack welds at distances equal to 6" from each end of the plate were performed to ensure contact of the two plates during the welding operation.

Temperature changes and transient thermal strains were measured during the experiments, using thermocouples and electric resistance strain gages respectively. Figure 2.1 shows the location of the instrumentation on both the top and bottom surfaces of the plate.

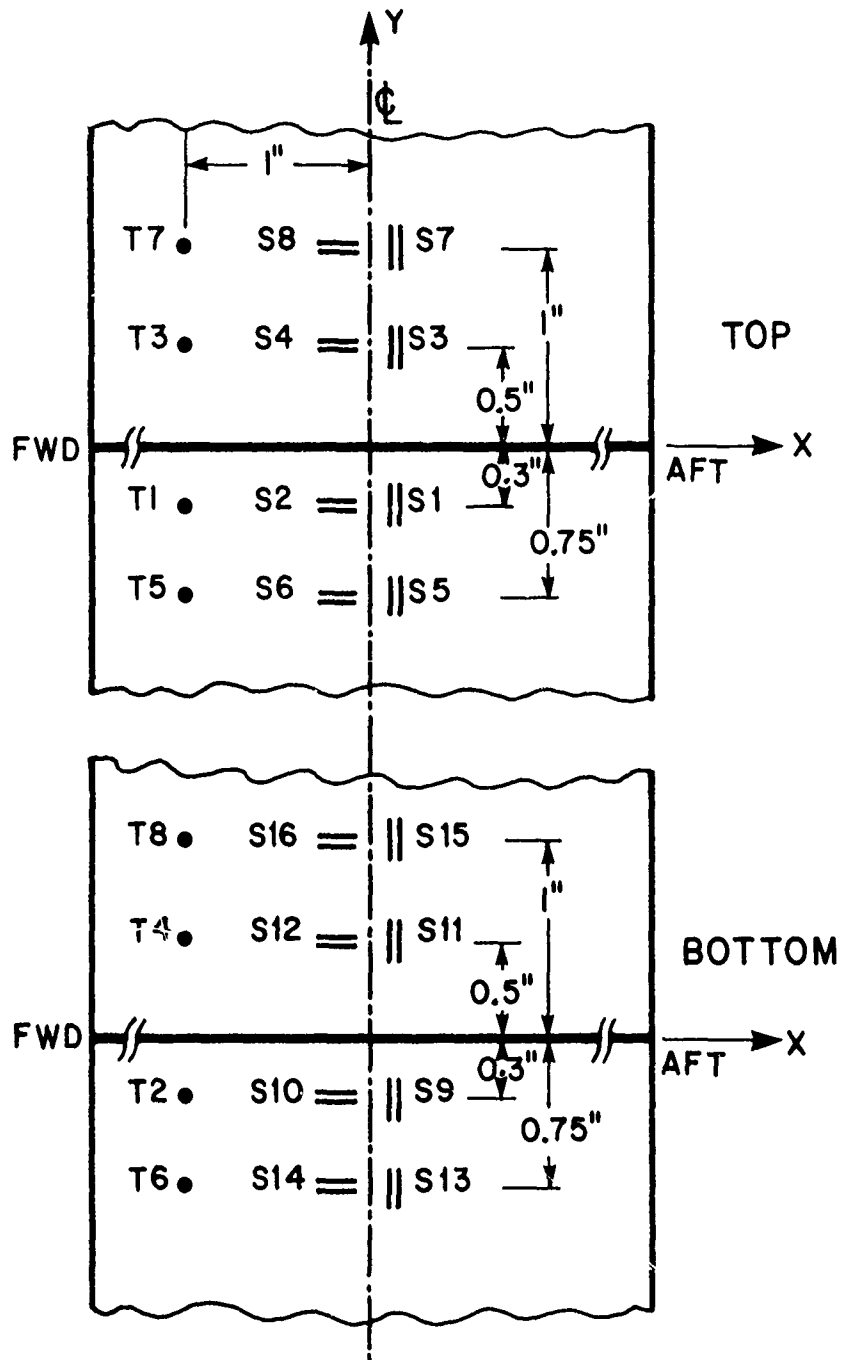
Figures 2.2 through 2.7 show representative results of the measurements of temperature and longitudinal strain changes. Also shown are results obtained using the M.I.T. one-dimensional computer program.³

The following observations can be made. First of all, the obtained results are very similar to the ones obtained during the previous investigations using EBW, something that shows the repeatability of such tests. Second, the one-dimensional computer program is not adequate for predicting transient strains in thick plates. This is mainly due to the fact that in such a case the transverse strains, which are neglected in the analysis, are of the same order of magnitude as the longitudinal ones. Finally, the calculated temperatures, using a variety of arc efficiencies, η_a , show good correlation only at locations away from the weld centerline; furthermore a uniform temperature is predicted through the plate thickness. Such behavior is the result of the line heat source assumption used in the one-dimensional program.

Triaxial distribution of residual stresses. The Rosenthal-Norton sectioning technique, described in the first progress report, was used to measure the triaxial distribution of residual stresses in the EB welded Plate.

Figure 2.8 shows the layout of the strain gages on the welded plate

³ Papazoglou, V.J., "Computer Programs for the One-Dimensional Analysis of Thermal Stresses and Metal Movement during Welding", M.I.T. OSP # 82558, January, 1977.



|| STRAIN GAGE (Y - DIRECTION)
== STRAIN GAGE (X - DIRECTION)
• THERMOCOUPLES

FIGURE 2.1 Location of thermocouples and strain gages on the top and bottom surfaces of the EB welded HY-130 plate.

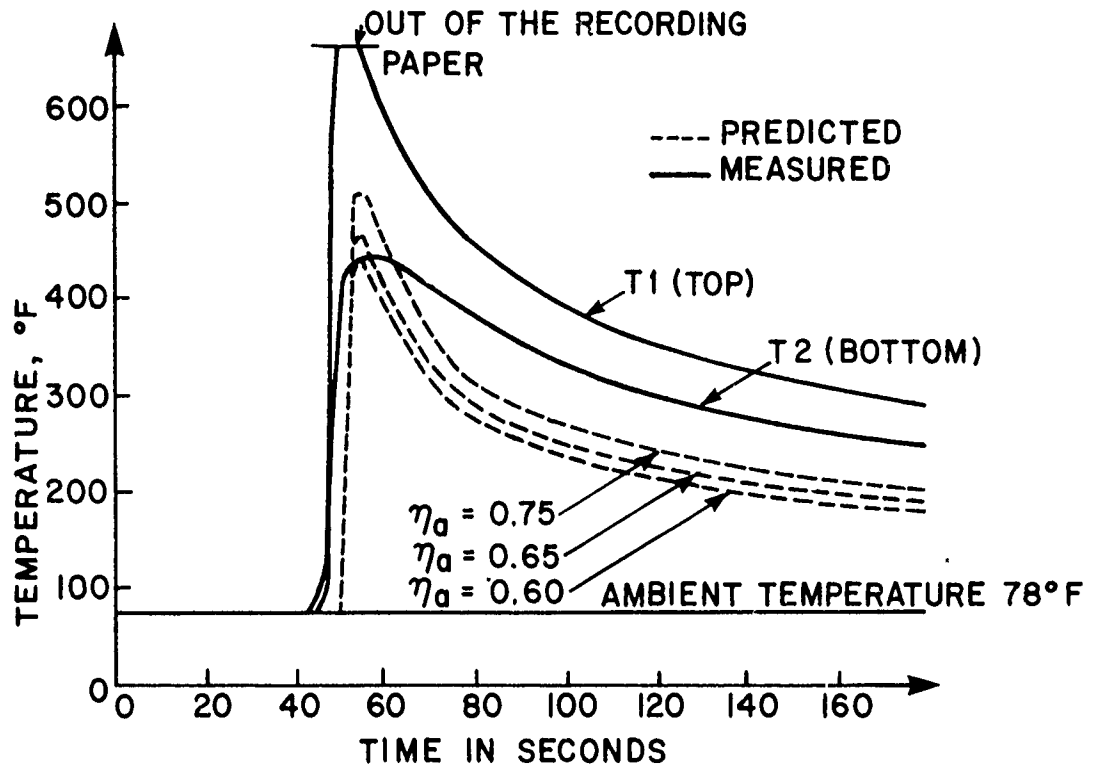


FIGURE 2.2 Measured and predicted temperature distribution at a point 0.3 in away from the weld centerline.

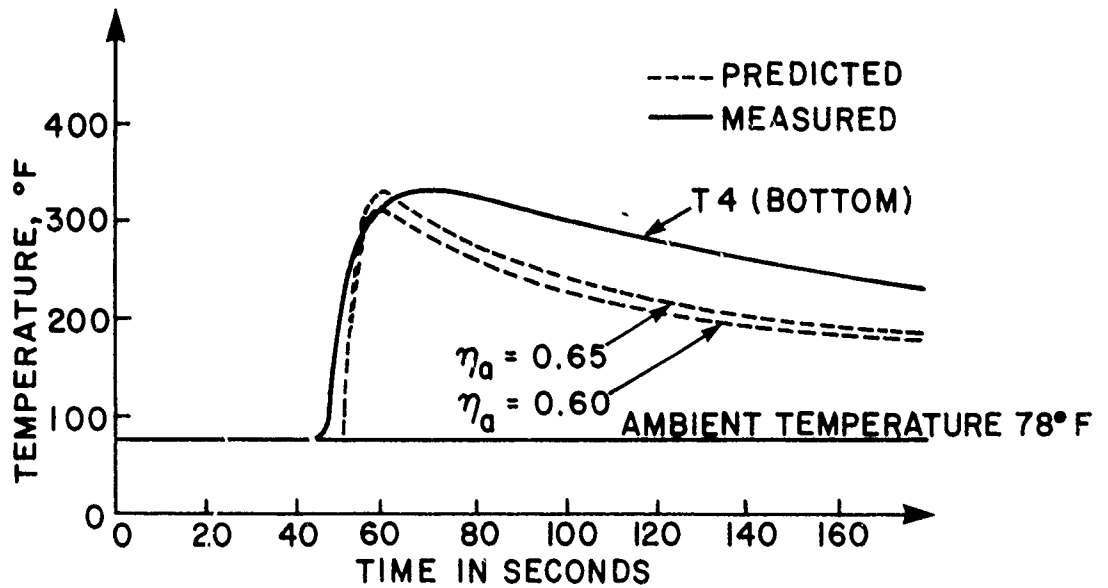


FIGURE 2.3 Measured and predicted temperature distribution at a point 0.5 in away from the weld centerline.

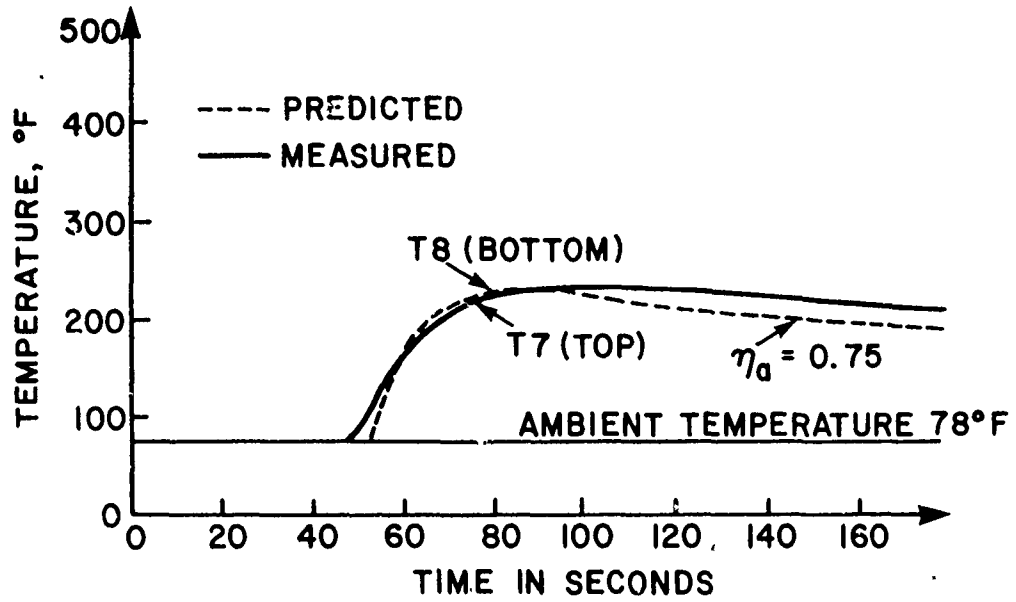


FIGURE 2.4 Measured and predicted temperature distribution at a point 1.0 in away from the weld centerline.

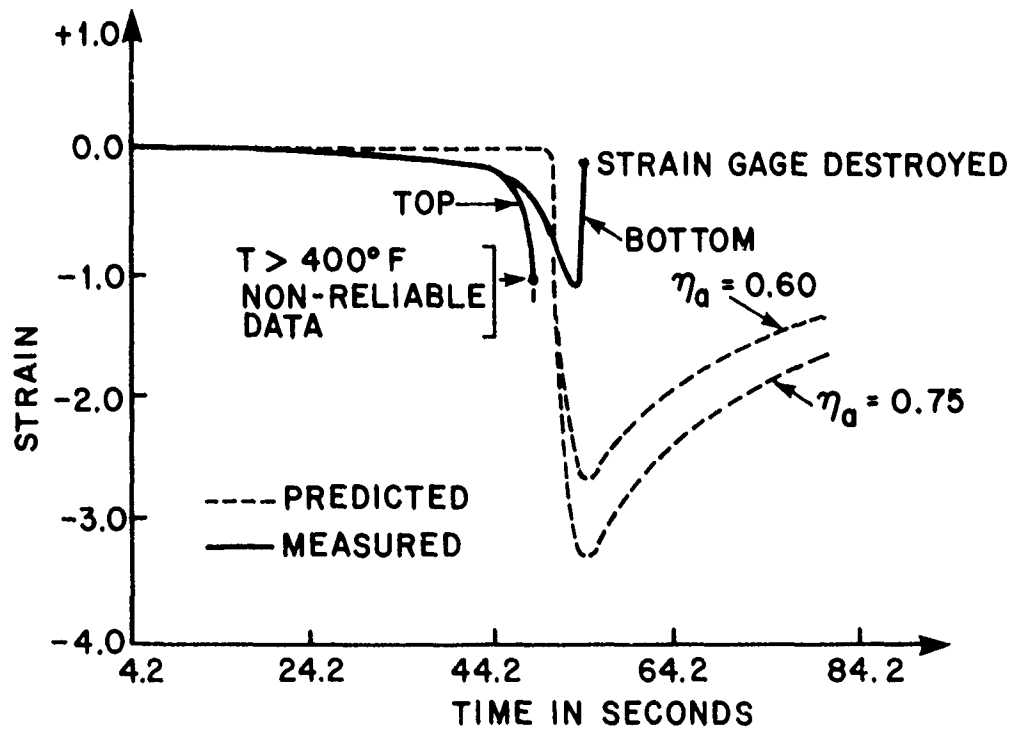


FIGURE 2.5 Measured and predicted longitudinal transient strain at 0.3 in away from the weld centerline.

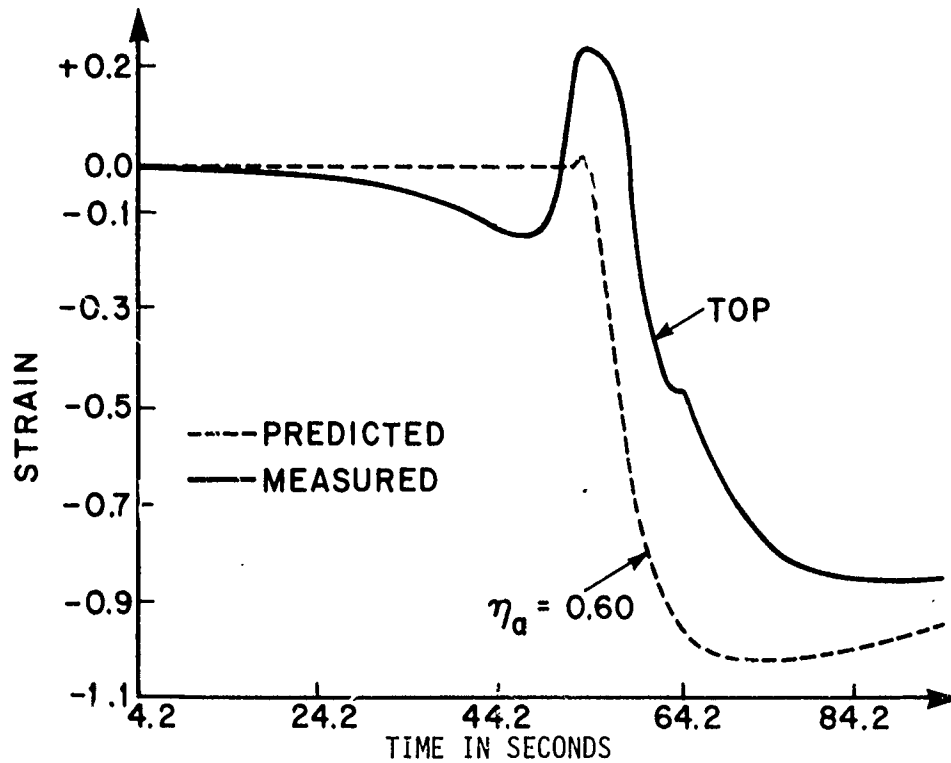


FIGURE 2.6 Measured and predicted longitudinal transient strain at 0.75 in away from the weld centerline.

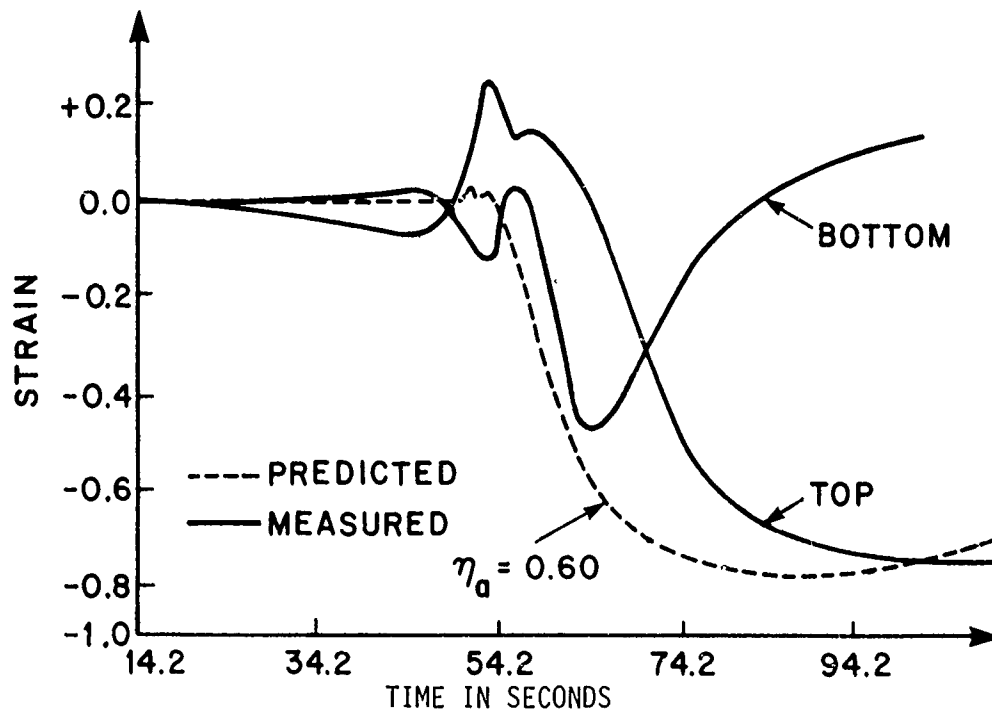


FIGURE 2.7 Measured and predicted longitudinal transient strain at 1.0 in away from the weld centerline.

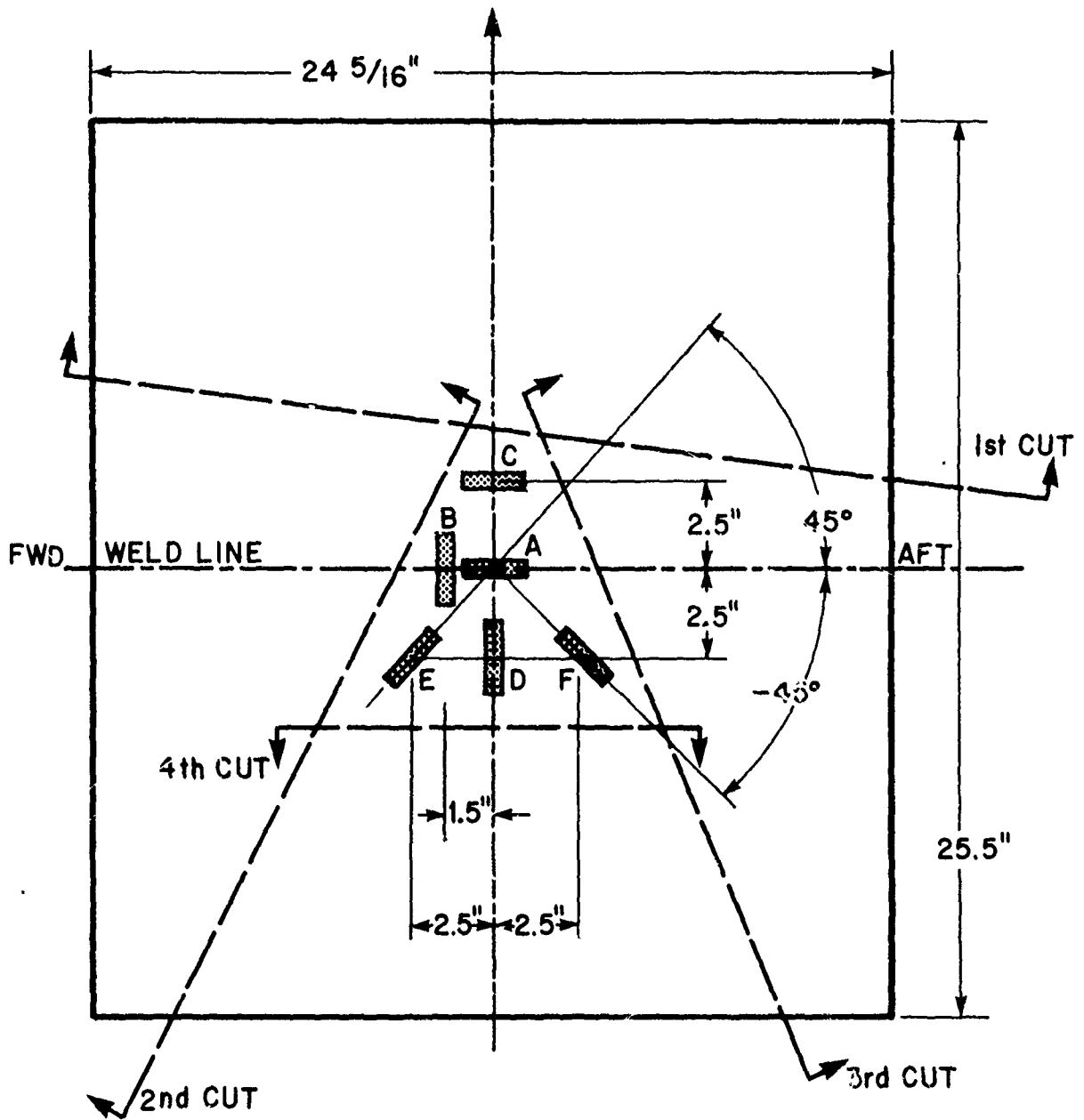


FIGURE 2.8 Layout of strain gages on the welded plate and illustration of basic cuts performed.

and illustrates the basic saw cuts performed. Figures 2.9 and 2.10 show the through thickness distribution of the longitudinal and transverse residual stresses, σ_x and σ_y , on the weld line. Figures 2.11 through 2.14 show the through thickness distribution of the longitudinal, σ_x , transverse, σ_y , shear τ_{xy} , and vertical, σ_z , residual stresses at a point 2.5 in. away from the weld line.

The obtained results seem to be consistent with results reported by other investigators. If compared with the results obtained in the 1020 steel investigation, as reported in the first progress report, several observations can be made. First, the stress levels encountered in the HY-130 specimen are much higher, as expected for a steel having a higher yield strength. Second, for both steels the maximum longitudinal residual stress, σ_x , on the weld centerline occurs at midthickness. Third, whereas the through thickness distribution of the transverse residual stress, σ_y , is rather smooth in the 1020 specimen, an abrupt and relatively high peak is observed in the HY-130 specimen at a point located at a distance equal to about 2/3 thicknesses from the top surface. This phenomenon, if true, can mean trouble as far as weld metal longitudinal cracking is concerned. Finally, it can be seen that at a point 2.5 in. away from the weld centerline very steep residual stress gradients are present for both σ_x and σ_y (see Figures 2.11 and 2.12). Such an occurrence was not observed in the 1020 steel specimen. It can be thus recommended that in future investigations on HY-130 steel the read-out of strain relaxations during the slicing operation of the measuring process should be more frequent, to more accurately establish the residual stress distribution.

2.3.2 GMA Welding Tests.

The welding and experimental measurement of the triaxial distribution of residual stresses was undertaken by Sousa Sa. A summary of this investigation's findings follow.

Welding procedure. Two HY-130 steel specimens were used having thickness of 7/8 in. and 1 in. and being 18 in. long and 32 in. wide.

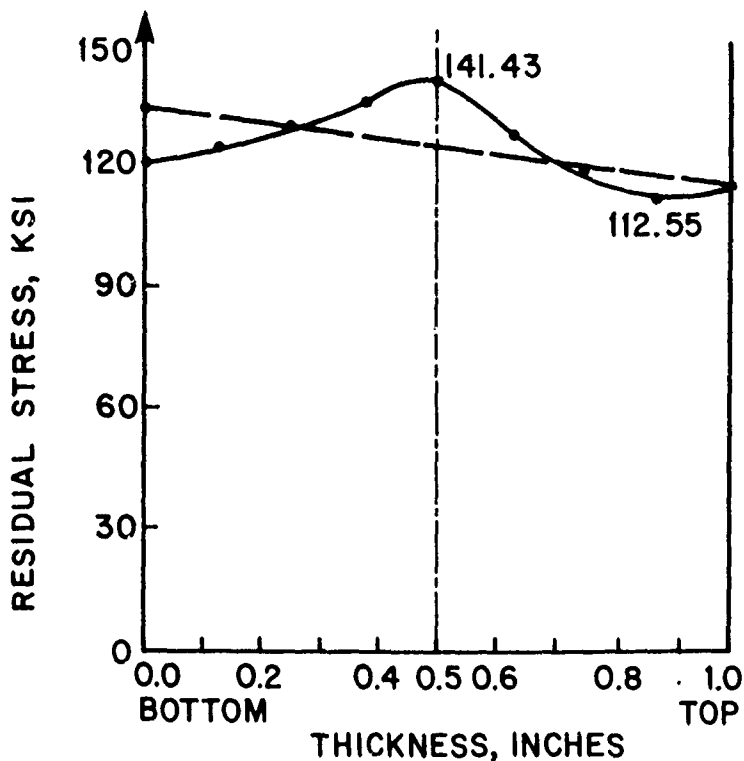


FIGURE 2.9 Through thickness distribution of the longitudinal residual stress σ_x on the weld centerline.

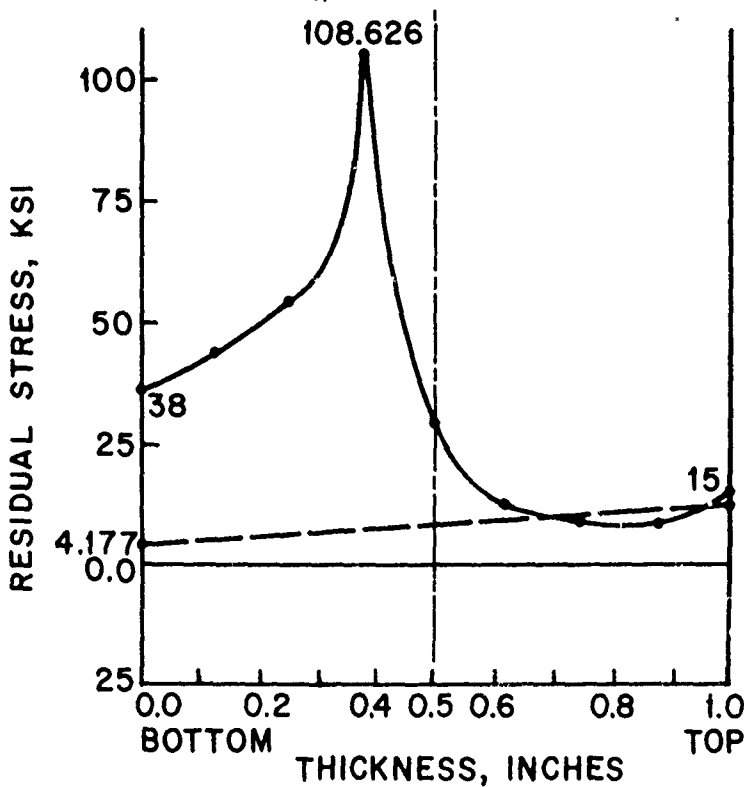


FIGURE 2.10 Through thickness distribution of the transverse residual stress σ_y on the weld centerline.

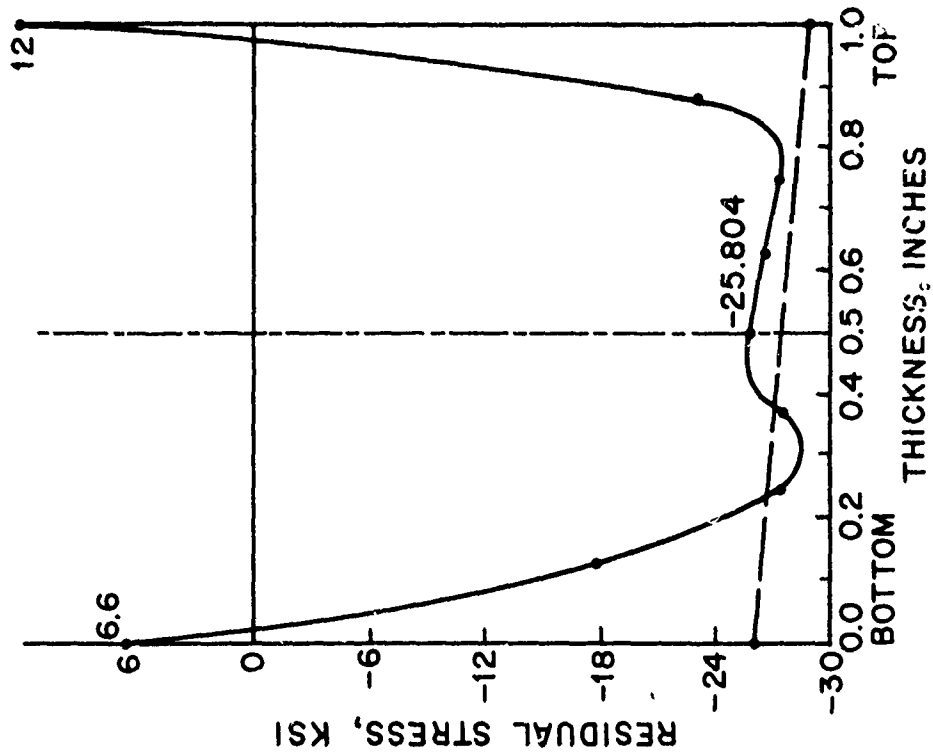


FIGURE 2.12 Through thickness distribution of the transverse residual stress, σ_y , at 2.5 in away from the weld centerline.

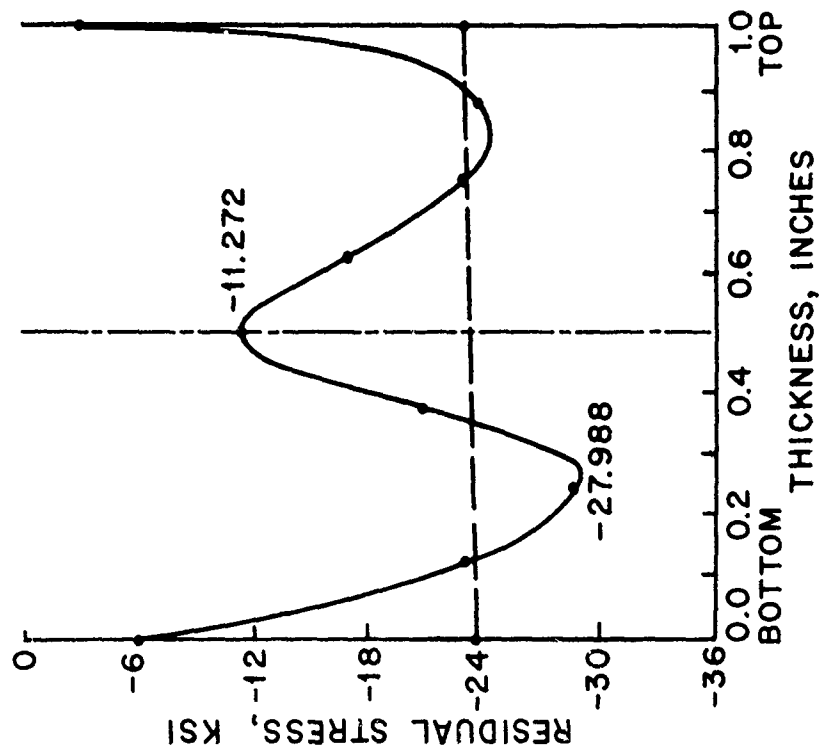


FIGURE 2.11 Through thickness distribution of the longitudinal residual stress, σ_x , at 2.5 in away from the weld centerline.

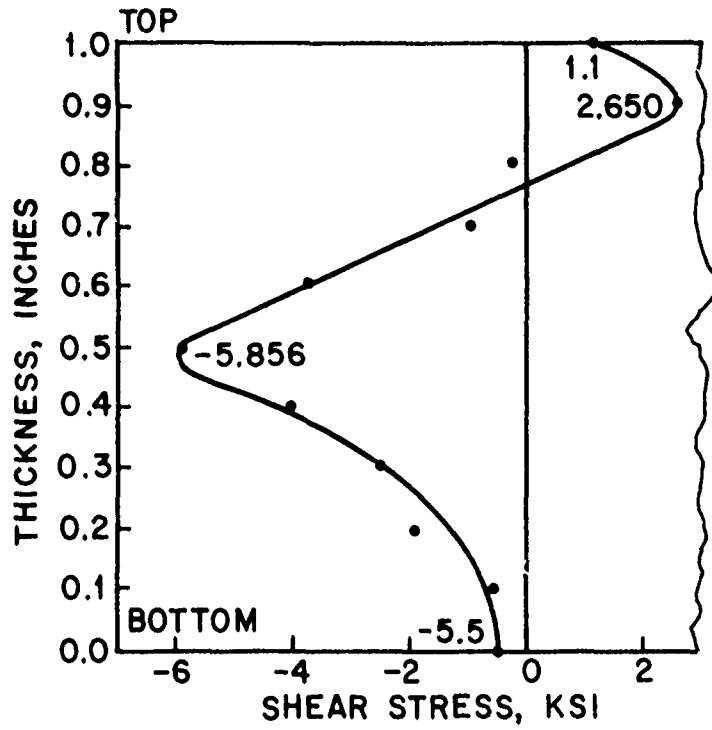


FIGURE 2.13 Through thickness distribution of the shear residual stress, τ_{xy} , at 2.5 in away from the weld centerline.

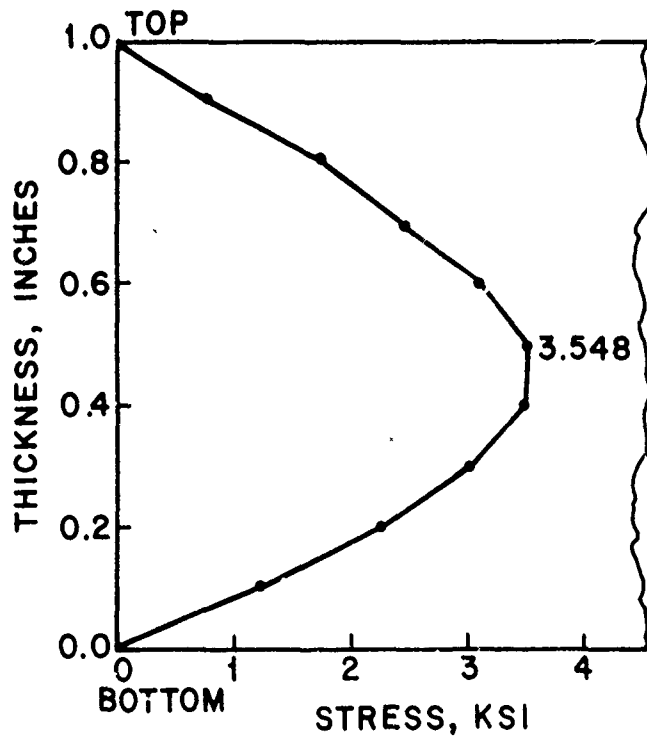


FIGURE 2.14 Through thickness distribution of the vertical residual stress, σ_z , at 2.5 in away from the weld centerline.

Welding was performed by the semi-automatic GMAW method; Table 2.1 details the parameters used.

TABLE 2.1
Welding Parameters

Process	GMAW
Polarity	DCRP
Weld type	Butt
Filler wire	1/16" LINDE 140 S
Shield gas	A + 2% O ₂
Gas pressure	30 psi
Pre-heating	150-200 °F
Wire speed	162 inches/min
Arc current	300 Amps
Arc voltage	28 volts
Arc speed	16 inches/min

The double-V groove was used for both specimens. Regarding the welding sequence, the one used for the 7/8 in. plate (Figure 2.15a) - consisting of completely welding the top and then the bottom side - resulted in an angular distortion equal to 3°. To avoid this type of distortion, the 1 in. thick specimen was welded using the sequence shown in Figure 2.16; no visible angular distortion was observed after this specimen cooled down to room temperature

Note that no temperature and transient strain histories were recorded during the welding operation since a considerable amount of data has already been accumulated on this subject during the other experiments of this research project.

Strain gage installation. After the specimens have cooled down to room temperature, a series of unidirectional strain gages was installed on both their top and bottom surfaces for the residual stress measurement according to the Rosenthal-Norton sectioning technique. Figure 2.17 shows

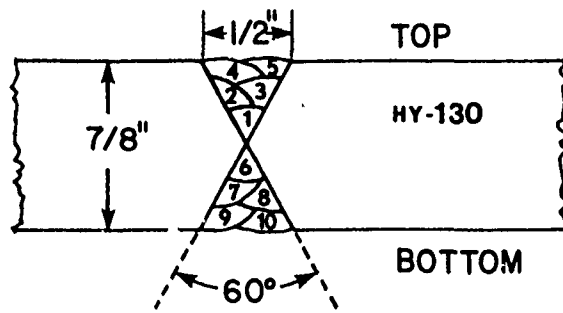


FIGURE 2.15a Groove dimensions and welding sequence for the 7/8" thick plate.

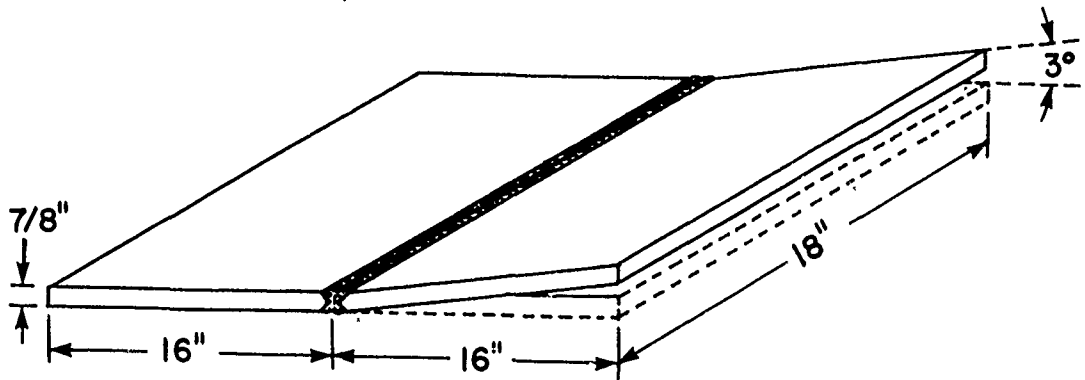


FIGURE 2.15b Irregular distortion obtained after welding the 7/8" thick plate.

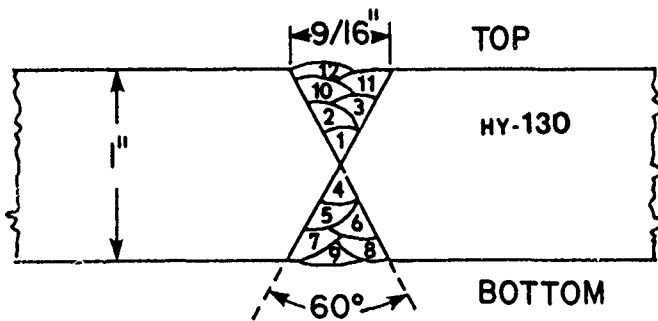


FIGURE 2.16 Groove dimensions and welding sequence for the 1" thick plate.

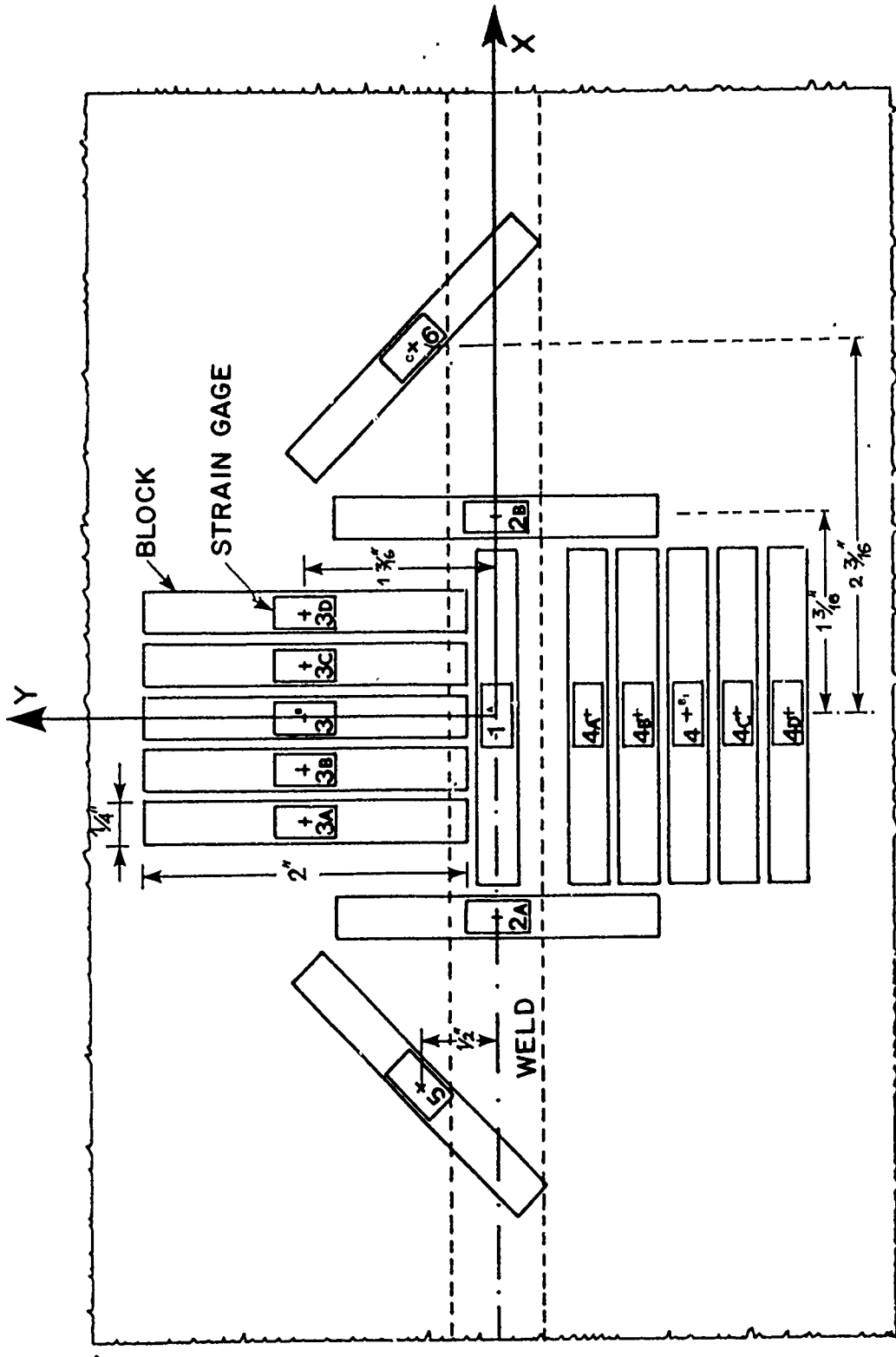


FIGURE 2.17 Strain gage arrangements for both plates.

the strain gage layout for the 7/8 in. specimen. A total of thirty gages, fifteen on each side, were used, numbered from 1 to 6: gages 1, 2A, and 2B for the measurement of the through-thickness distribution of the longitudinal, σ_x , and transverse, σ_y , residual stresses on the weld line; gages 3, 3A through 3D and 4, 4A through 4D for the measurement of σ_x and σ_y at a distance 1 3/16 in. from the weld line at mid-plate; and gages 5 and 6 for the measurement of the shearing stress, τ_{xy} , at $x = 2 \frac{3}{16}$ in., $y = \frac{1}{2}$ in.

Some explanation is in order at this point for the use of five longitudinal and five transverse strain gages on each plate surface at a distance equal to 1 3/16 in. from the weld line. Experience gained from previous tests has indicated that it is very difficult to accurately measure the strain relieved during the last stages of the slicing operation of the measurement procedure because of the small size of the remaining sliced blocks. Based on that, blocks 3A through 3D (and similarly 4A through 4D) would be used to measure these relieved strains by cutting thin slices from the top and bottom surfaces of the whole blocks; the released strain that would have been measured from block 3 (and similarly 4) could then be found through interpolation from the already obtained values. At the same time, and for comparison purposes, the strain release from the last slicing of block 3 (and 4) would also be measured.

The strain gage layout on the 1 in. specimen was similar, the only difference being that strain gages 3A through 3D and 4A through 4D were skipped. This was due to the fact that the comparison referred to in the previous paragraph was favorable; it was thus decided that the additional eight gages on each surface were not necessary.

Measurement procedure. The blocks, represented by the larger rectangles in Figure 2.17, with the strain gages on their top and bottom surfaces, were first cut free from the plates using a band saw. These blocks were then each split in half with the aid of a circular diamond saw mounted on a "Sanford" surface grinder provided with a magnetic chuck. The same saw was used for the subsequent block slicing which was aided by the specially built holding device shown in Figure 2.18

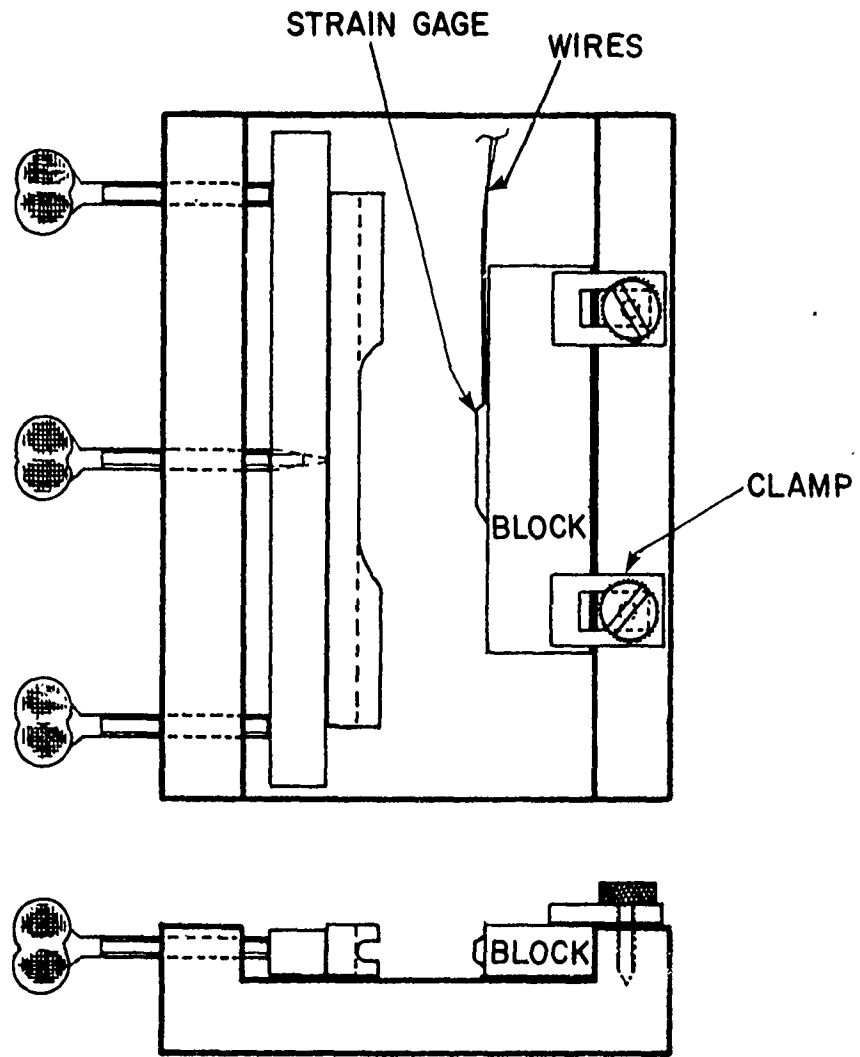


FIGURE 2.18 Holding device with block prepared for slicing.

The blocks from the 7/8 in. thick plate were sliced in 1/8 in. thick slices. Upon studying the observed results, however, and due to their oscillatory nature, it was decided that the 1 in. thick plate would be sliced at every 1/16 in.

Results. Figures 2.19 and 2.20 show the through thickness distribution of the longitudinal, σ_x , and transverse, σ_y , residual stresses respectively on the weld line for both the HY-130 GMA welded plates; also shown, for comparison purposes, are the results obtained by Mylonas⁴ on the 1020 EB welded plates and by Coumis⁵ on the HY-130 EB welded plate. A close examination of these two figures reveals several facts. First, the maximum values of residual stress are much higher in the HY-130 than in the 1020 mild steel. This is to be expected from the much higher yield strength of the HY-130 steel. Second, the through thickness distribution of σ_x in the EB welded specimens is more uniform. The GMAW process results in a wavy and irregular distribution with low tensile or even compressive stresses at both top and bottom weld surfaces and high tensile stresses, approaching yield strength, at around mid-thickness. This is believed to be primarily due to the multipass nature of the GMAW process. Third, with regard to σ_y , an alteration between tension and compression is observed in the GMA welded specimen, whereas the EB specimens show tension everywhere. Such a behavior can again be attributed to multipass effects. Finally, it seems reasonable to state that the welding sequence in GMAW does not radically alter the thickness distribution of both σ_x and σ_y .

Figures 2.21 and 2.22 present the through thickness distribution of σ_x and σ_y respectively at a point 1 3/16 in. away from the weld line for both HY-130 GMA welded specimens. As it can be seen the magnitudes of both σ_x and σ_y are not surprisingly much lower than the respective ones on the weld line.

⁴For details see first technical progress report of this research program dated Nov. 30, 1979 (Section 2.6).

⁵For details see Section 2.3.1 of this progress report.

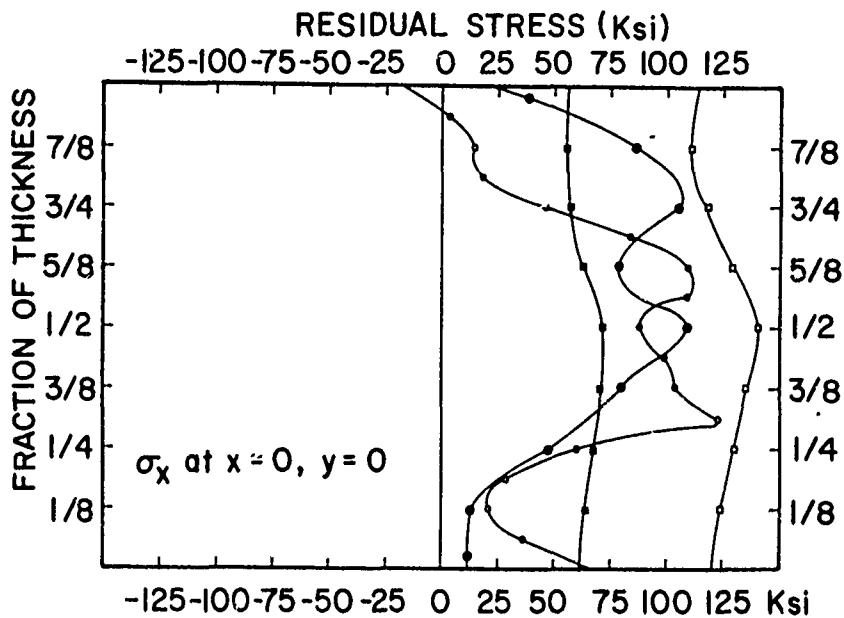


FIGURE 2.19 Through thickness longitudinal residual stress, σ_x , distribution on the weld line.

BOTH FIG. 2.19 & 2.20

- HY-130, GMAW, $t = 7/8''$ (Sa)
- HY-130, GMAW, $t = 1''$ (Sa)
- 1020 St, EBW, $t = 1''$ (Mylonas)
- HY-130, EBW, $t = 1''$ (Coumis)

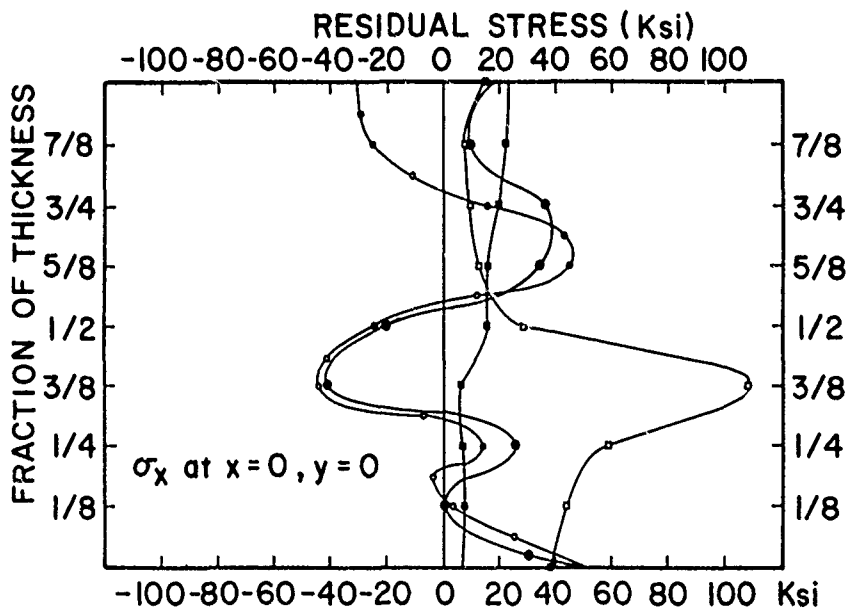


FIGURE 2.20 Through thickness transverse residual stress, σ_y , distribution on the weld line.

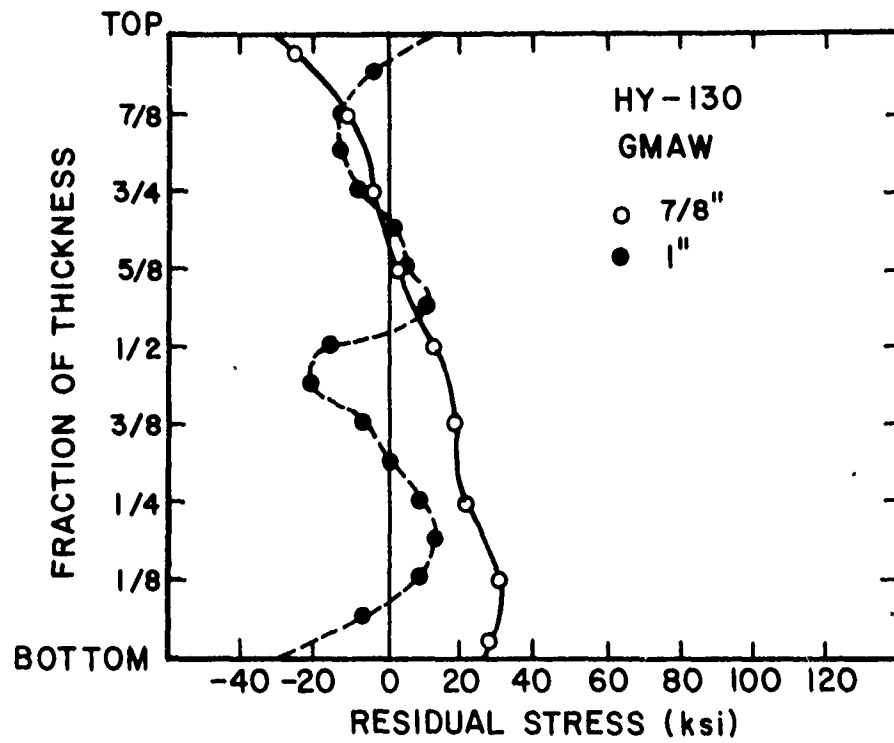


FIGURE 2.21 Through thickness longitudinal residual stress, σ_x , distribution 13/16" away from weld line.

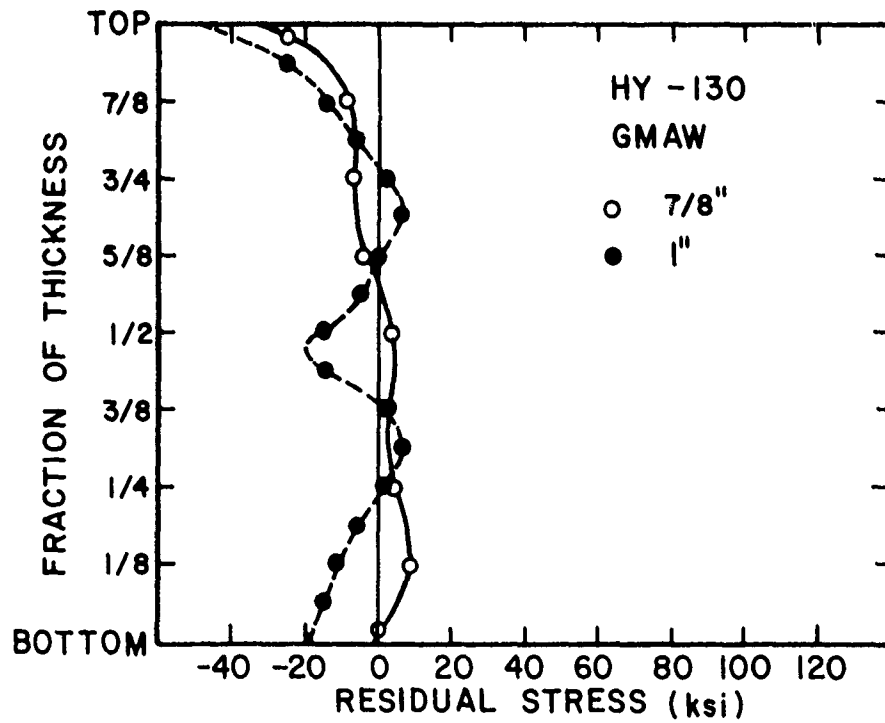


FIGURE 2.22 Through thickness transverse residual stress, σ_y , distribution 13/16" away from weld line.

Through thickness distributions of the shearing, τ_{xy} , and vertical, σ_z , residual stresses were also calculated but are not recorded here because of their insignificantly low values.

2.4 Experiments on Simple Restrained Butt Welds (Step 1.6).

This section covers the continuation of Step 1.6 which has been initiated during the second year of this research program. The following thesis, dealing with this step, has been completed:

Goncalves, E., "Investigation of Welding Heat Flow and Thermal Strain in Restraint Steel Plates", S.M. Thesis, M.I.T., May 1980.

2.4.1 Experimental Procedure

The specimen configuration for this series of experiments is shown in Figure 2.23. A total of nine similar specimens were used as detailed in Table 2.2. The welding was performed using the GMAW process; the welding conditions are given in Table 2.3. Figure 2.24 shows the welding sequence.

TABLE 2.2
Description of Restrained Specimens

<u>Specimen No.</u>	<u>Material</u>	<u>Thickness (in.)</u>	<u>B (in.)</u>	<u>Number of Passes</u>
1	SAE 1020	1/2	18	7
2	"	1/2	12	7
3	"	1	18	13
4	"	1	12	13
5	"	2	18	40
6	"	2	12	40
7	HY-130	7/8	18	10
8	"	7/8	12	10
9	"	2	12	40

Note: B is defined in Figure 2.23

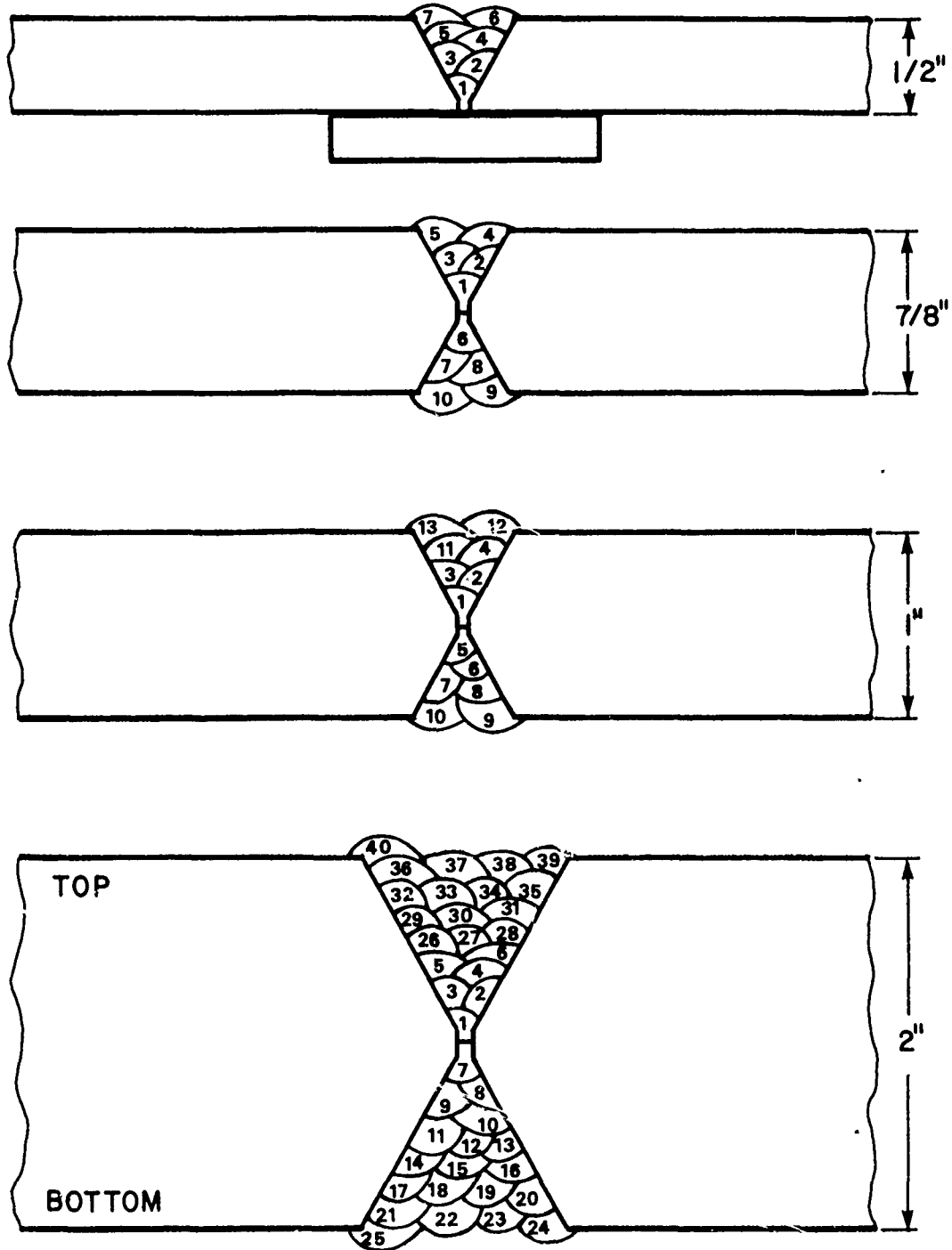


FIGURE 2.24 Welding sequence.

TABLE 2.3

<u>Welding Conditions for the Restrained Specimens</u>		
	<u>SAE 1020</u>	<u>HY-130</u>
Process	GMAW	GMAW
Polarity	DCRP	DCRP
Weld Type	Butt	Butt
Filler Wire	1/16" A681	1/16" LINDE 140
Shield Gas	A + 2%O ₂	A + 2%O ₂
Gas Pressure	30psi	30psi
Pre-heating	150°-200°F	150°-200°F
Wire speed	162 in/min	162 in/min
Arc Current	280A	300A
Arc Voltage	28V	28V
Arc Speed	15-18 in/min	15.8 in/min

Both temperature changes and transient strains were measured during the welding process. The location of the thermocouples and electric resistance strain gages used for these measurements are given in Figure 2.25.

Finally, the joint transverse shrinkage was measured after each welding pass using a clip gage.

2.4.2 Results

Goncalves' thesis contains a significant amount of curves showing the results obtained during the experiments. Figures 2.26 through 2.32 provide some representative graphs for the temperature and thermal strain variations.

The temperature distributions can be seen to be expected. Regarding the distributions of the longitudinal transient strain, SX, they seem to follow the same pattern in all experiments; at the point closer to the weld line the strain curves are initially constant, decrease a little until reaching a minimum, increase abruptly to a maximum higher than the initial

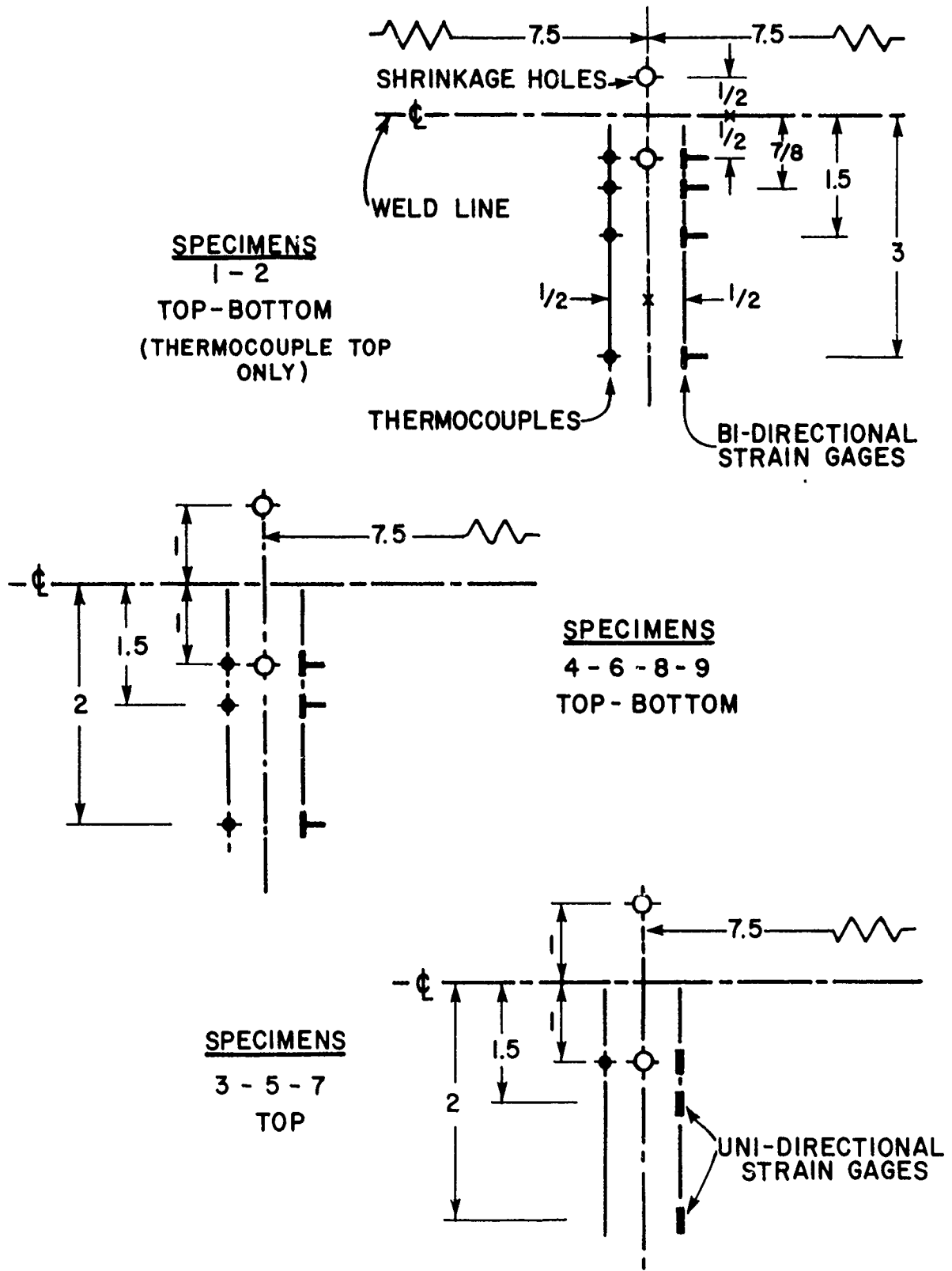


FIGURE 2.25 Thermocouples, strain gages and shrinkage reading positions.

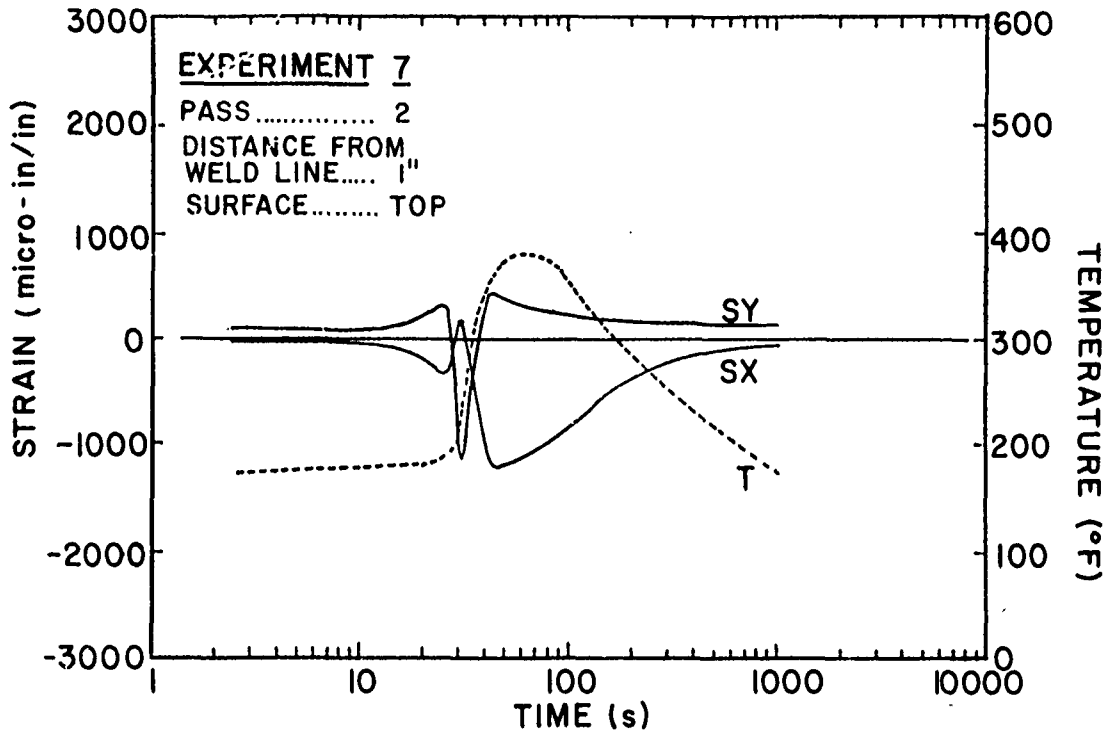


FIGURE 2.26 Temperature (T) and thermal strains in x (SX) and y (SY) directions.

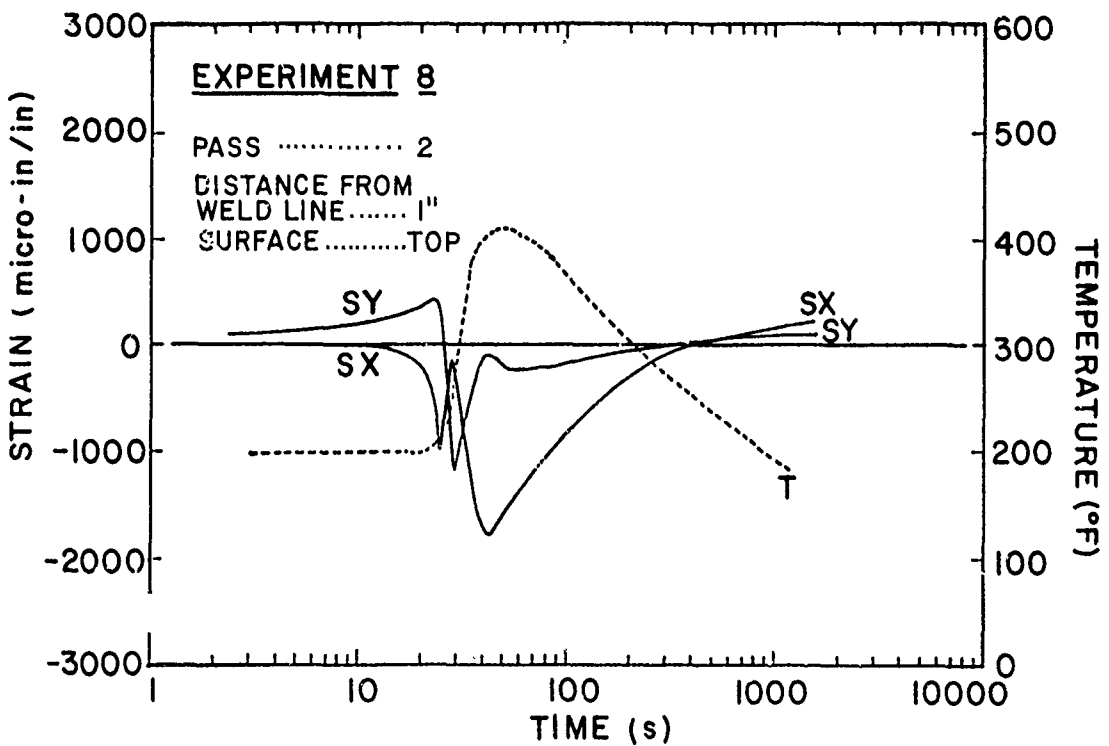


FIGURE 2.27 Temperature (T) and thermal strains in x (SX) and y (SY) directions.

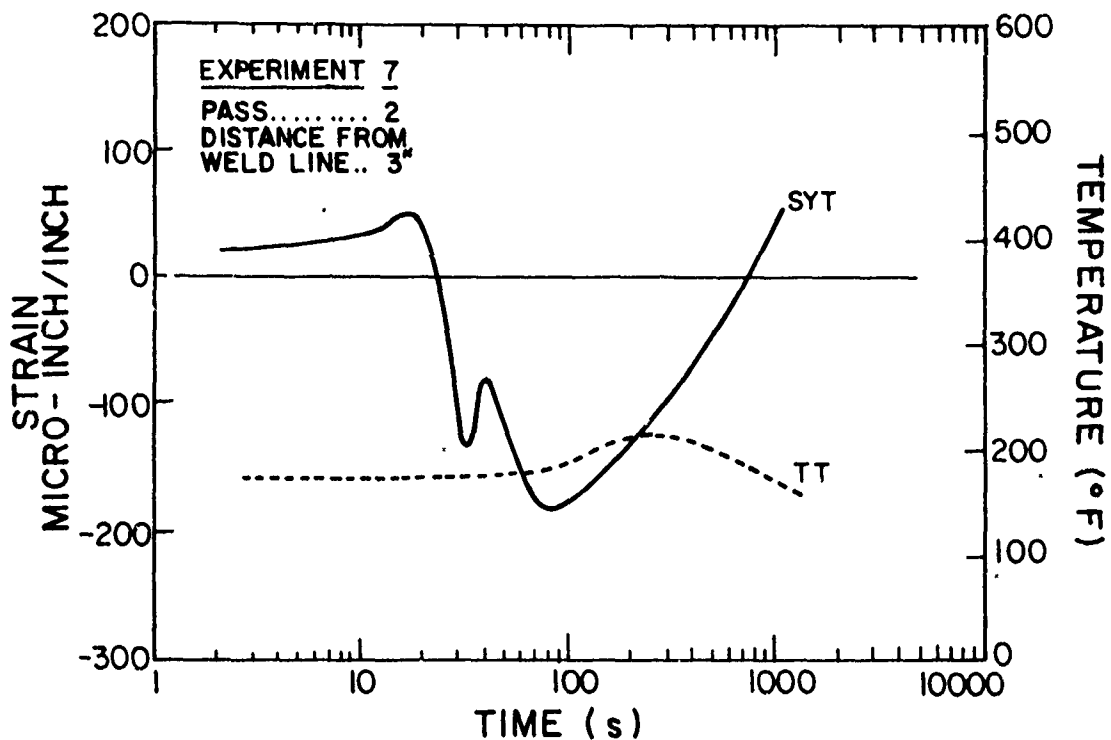


FIGURE 2.28 Temperature on the top surface (TT) and thermal strains in the y direction on top and bottom surfaces (SYT, SYB).

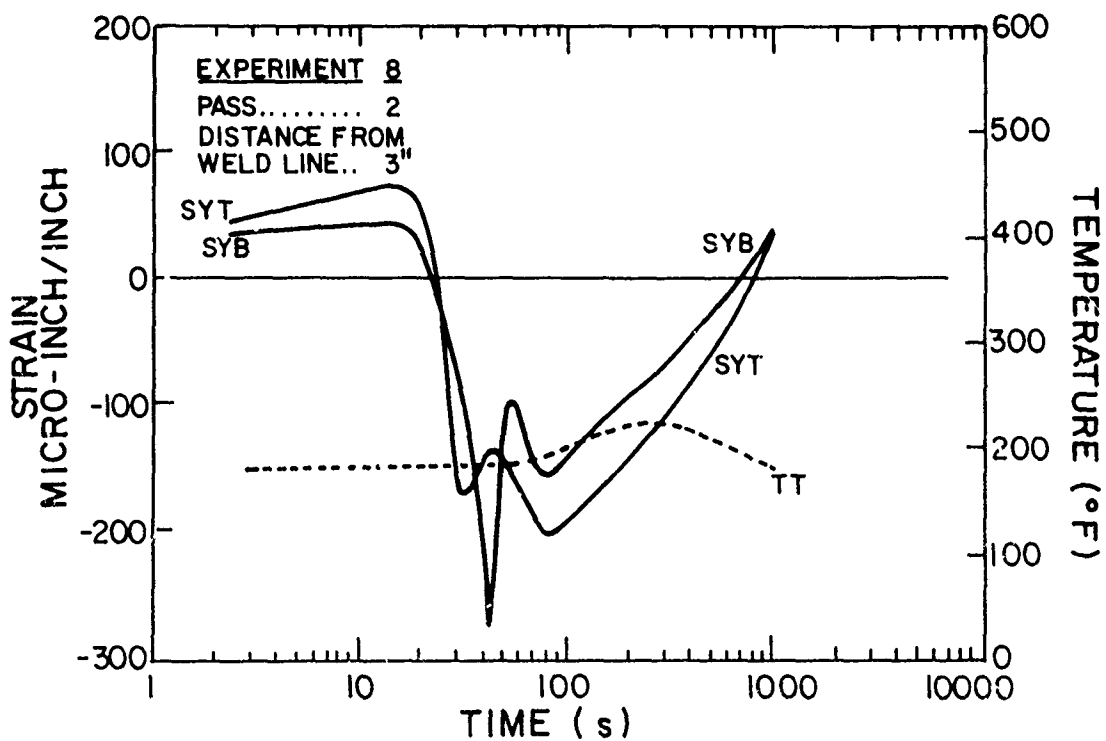


FIGURE 2.29 Temperature on the top surface (TT) and thermal strains in the y direction on top and bottom surfaces (SYT, SYB).

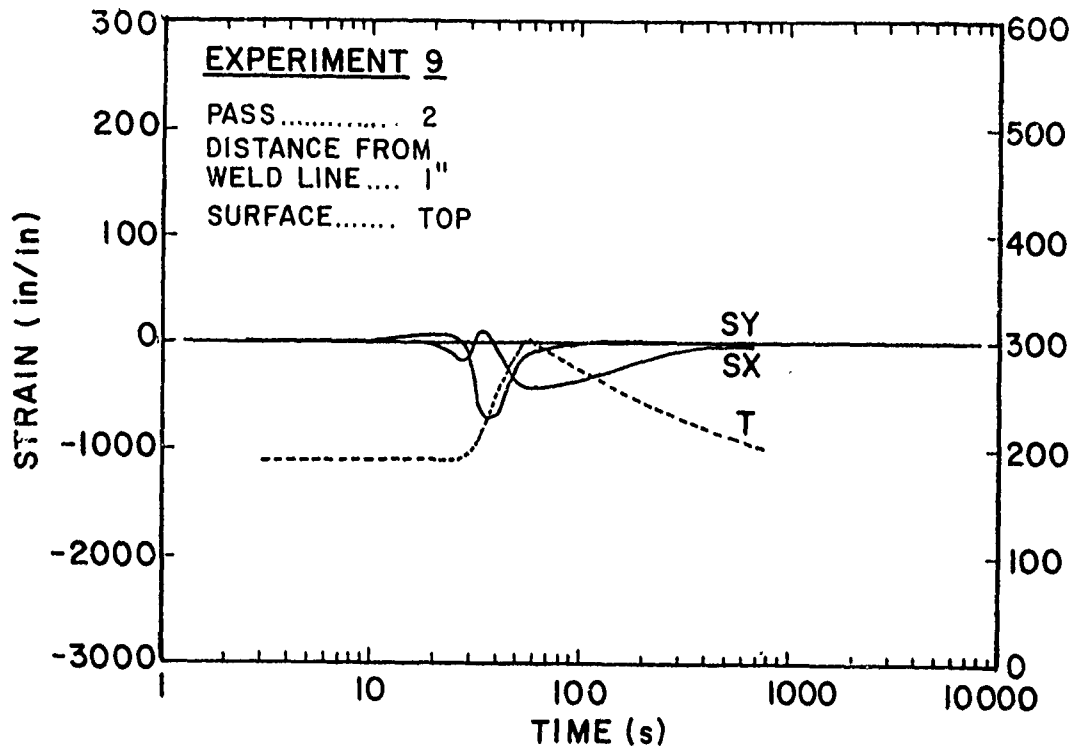


FIGURE 2.30 Temperature (T) and thermal strains in x (SX) and y (SY) directions.

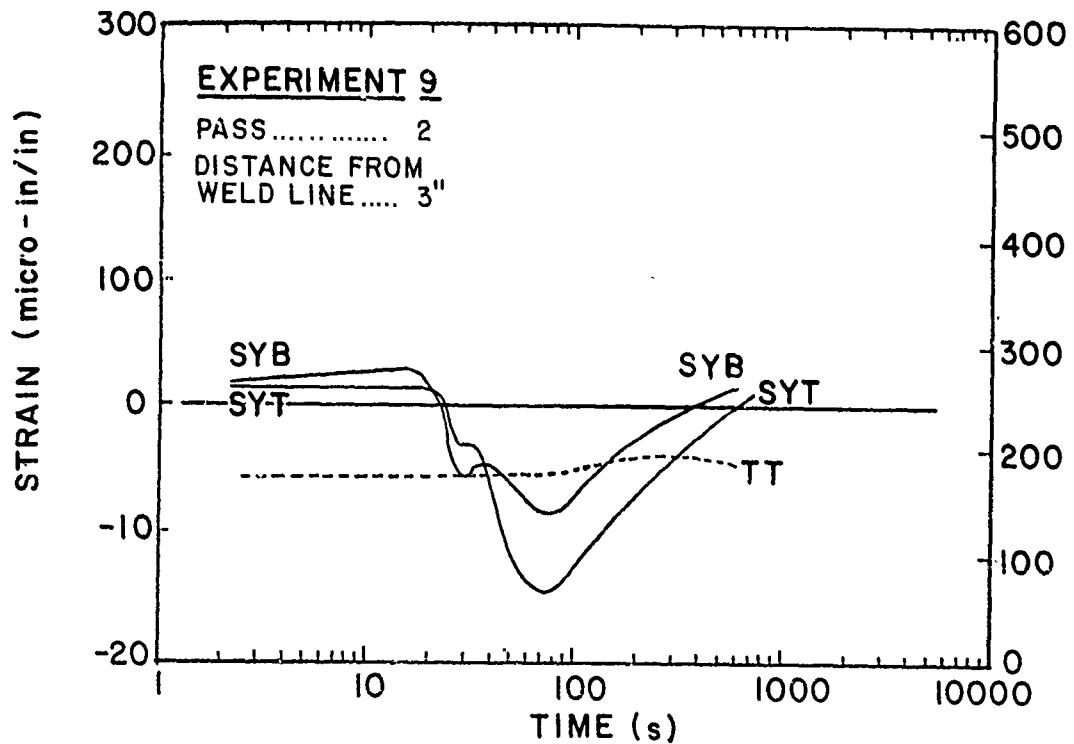


FIGURE 2.31 Temperature on the top surface (TT) and thermal strains in the y direction on top and bottom surfaces (SYT, SYB).

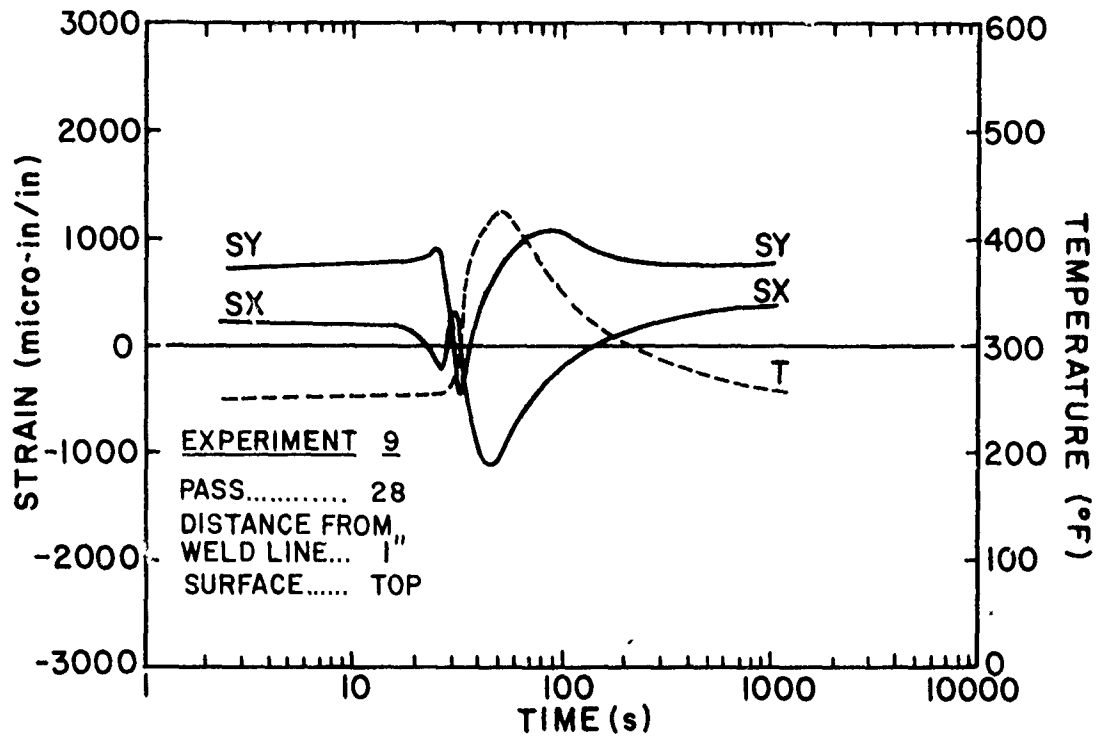


FIGURE 2.32 Temperature (T) and thermal strains in x (SX) and y (SY) directions.

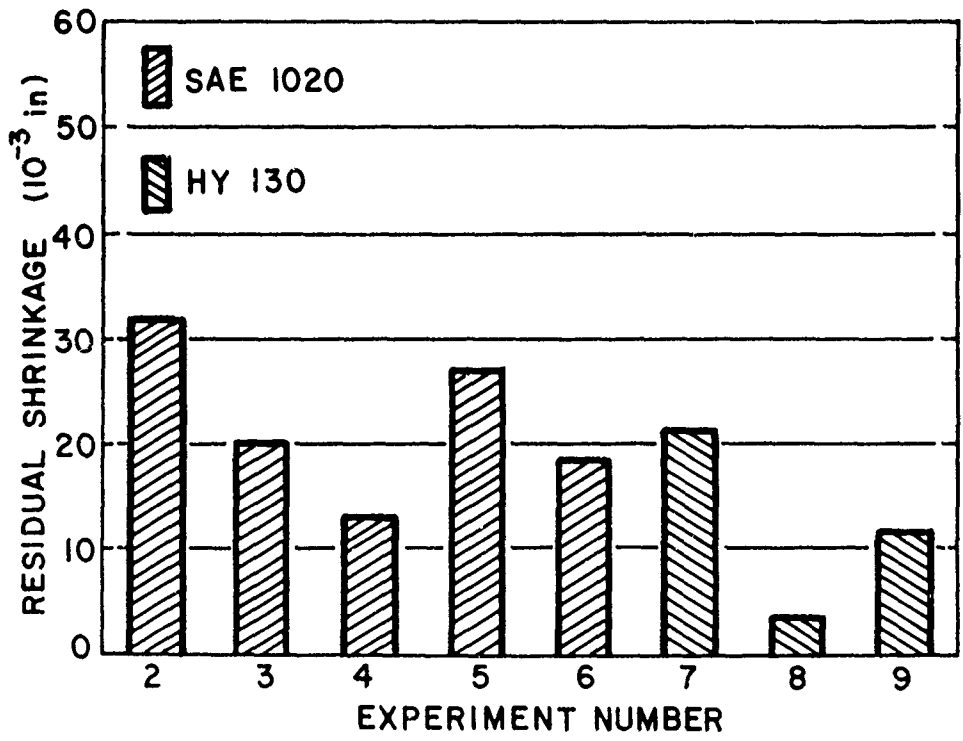


FIGURE 2.33 Residual shrinkage after last pass in different experiments.

value, decrease again to a second minimum, in general lower than the first one, and finally increase asymptotically towards a constant value. As far as the transverse transient strain, S_Y , is concerned, the pattern is similar but in reverse order, i.e., there is now a minimum between two maxima.

Finally, Figure 2.33 shows the residual transverse shrinkage after the last pass in the different experiments performed.

2.5 Experiment on Restrained Cracking Test Specimen (Step 1.9).

The following thesis, dealing with Step 1.9, has already been completed:

Suchy, A.F., "Investigation of Temperature Distribution and Thermally Induced Transient Strains in Highly Restrained, Thick, HY-130 Steel Plate Weldments", Ocean Engineer Thesis, M.I.T., June 1980.

A summary of the results appearing in this thesis is presented below.

2.5.1 Description and Experimental Procedure.

The restrained cracking specimen used for the window test is intended to provide a severe degree of restraint in which to check, in a go-no-go fashion, whether HY-130 steel can be successfully welded without cracking, Figure 2.34 gives the design of the specimen, whereas Figure 2.35 shows the standard X-groove configuration for the test and the one used for the experiment conducted at M.I.T. The reason for the smaller separation of plates in the M.I.T. experiment was the lack of GMA filler wire for HY-130 steel with diameter larger than 1/16".

The restraining base plate was made of SAE 1020 mild carbon steel and not of HY-130 steel since its sole purpose is to anchor the HY-130 plates that will be butt welded. These two plates were first fillet welded on the base plate using the shielded metal arc process. Table 2.4 provides the welding conditions used.

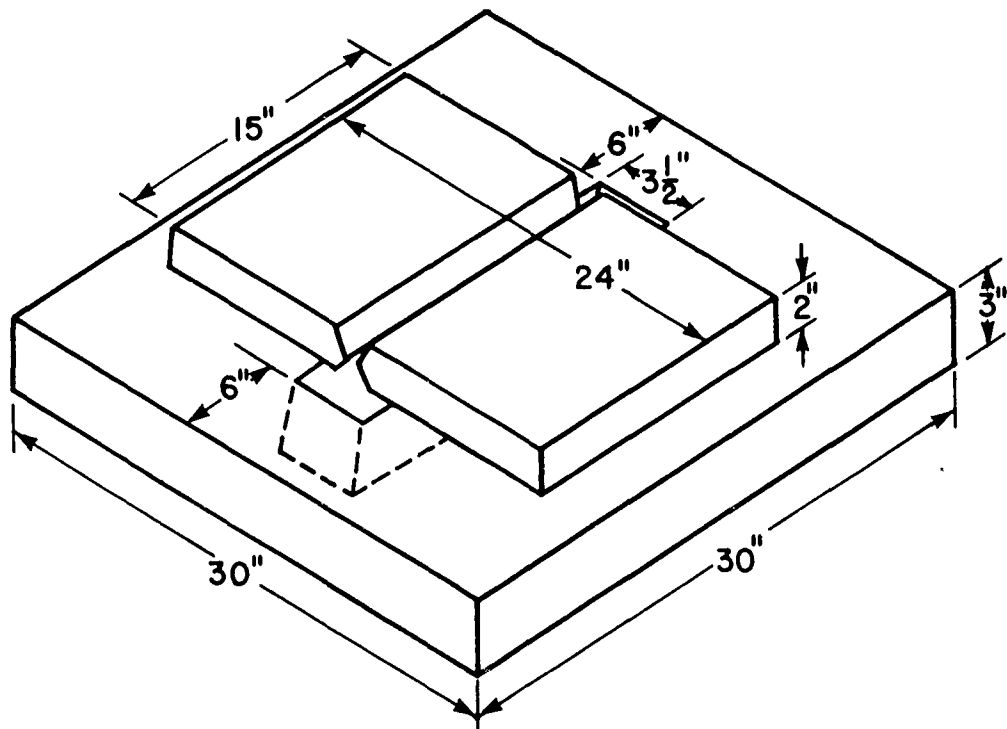


FIGURE 2.34 Window specimen design.

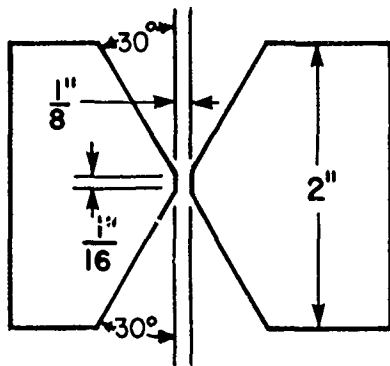


FIGURE 2.35a X-groove configuration
Mare Island tests.

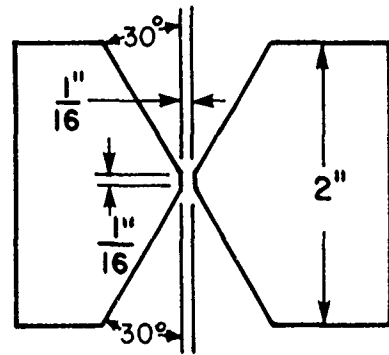


FIGURE 2.35b X-groove configuration
M.I.T. test.

The first pass of the butt welding was performed again using the SMAW process, whereas the subsequent 35 passes were done with the GMAW process. Table 2.4 gives the welding conditions used. The top side was welded first in 17 passes; the plate was then flipped over and 19 more passes were laid to complete the joining (a total of 36 passes).

Temperature changes and transient thermal strains were measured during the whole welding operation via thermocouples and strain gages, the locations of which are shown in Figures 2.36 and 2.37.

TABLE 2.4

Welding Conditions for the Window Specimen			
Base metals	1020 to HY-130	HY-130	HY-130
Weld Type	Fillet	Butt	Butt
Process	SMA	SMA	GMA
Polarity	DCRP	DCRP	DCRP
Arc Volts	30	30	28
Arc Amps	275	140	300
Travel Speed (ipm)	12	12	16
Heat Input (KJ/in)	41.25	21	31.5
Filler Wire	---	---	1/16" LINDE-140
Electrode	5/32" MIL-14018	5/32" MIL-14018	---
Shielding Gas	---	---	98% Argon, 2% Oxygen
Number of Passes	3	1	35
Preheat-Interpass Temperature	250°F	250°F	250-300°F. Interpass temp. meas. at outermost thermo- couple.

2.5.2 Results

Suchy's thesis contains the results of 20 of the 36 passes in both graphical and tabular form for further reference. Some selected results will be included in this section.

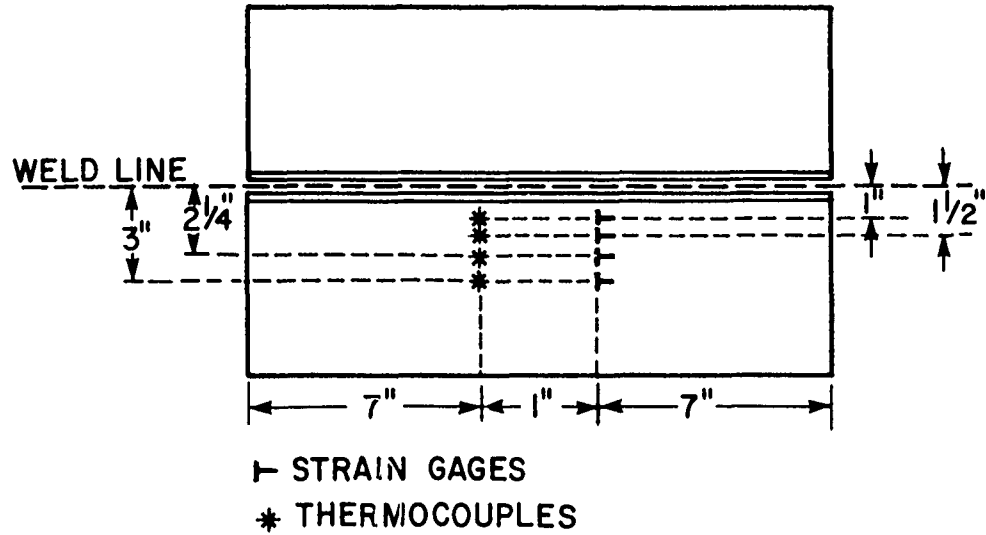
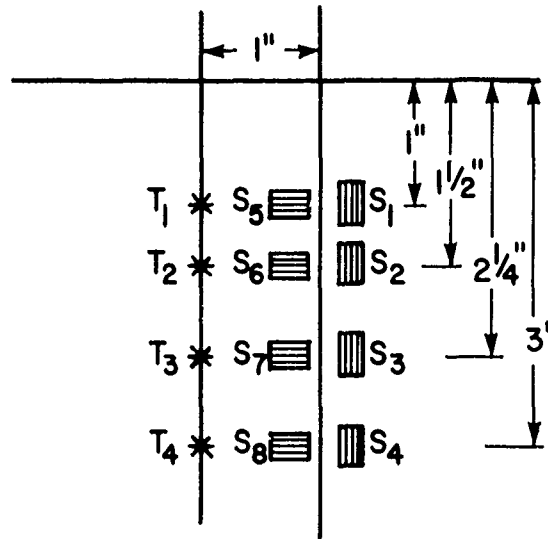


FIGURE 2.36 Strain gage and thermocouple placement on test plate.



- T₁ through T₄ thermocouple locations
- S₁ through S₄ transverse strain gage locations
- S₅ through S₈ longitudinal strain gage locations

FIGURE 2.37 Strain gage and thermocouple designations and locations on test plate. These designations are used to identify measurements plotted on curves.

Figures 2.38 through 2.41 show the temperature histories measured during pass numbers 1, 17, 18, and 36. These passes were selected because after pass 17 the plate was flipped over; pass 36 was the last welding pass. It can be seen that in all instances the thermocouples located furthest away from the weld centerline, T_3 and T_4 , show little temperature change within the time frame of the plots. The same occurs with the closest located thermocouples, T_1 and T_2 , during passes 18 and 36; this latter is due to the fact that the thermocouples are located on the opposite surface from that on which the welding is performed.

Figures 2.42 and 2.43 show the transverse transient strain distribution for passes 1, 13, 17, 18, 27, and 35 at the two measuring points closest to the weld line respectively. The same distributions but for the longitudinal transient strains are presented in Figures 2.44 and 2.45. Finally, Figure 2.46 shows the longitudinal transient strain history for the last six weld passes analyzed at 1 in. away from the weld centerline. It can be seen that the results obtained were similar to the ones obtained in other experiments conducted by investigators both at M.I.T. and elsewhere. In other words, the longitudinal strains were always higher than the transverse ones; phase transformation effects in the strain distributions were evident at the points closer to the weld line; and the magnitude of strains increased as more passes were being laid, because of the increase in the degree of restraint.

2.6 Measurement of Strain Energy Release on Specimens Made in 1.6 and 1.9 (Step 1.10)

The crack opening displacement (COD) was measured on the specimens welded in Step 1.6. The measurement was made using a clip gage. Since no external stress field was applied during the experiment, the required notch and its propagation was simulated by a saw cut (using a round saw). Furthermore, since the crack propagation was taking place in a residual stress field, strain gages were installed around the crack to measure the strain relaxations that would take place, from which the residual stress relaxations could be calculated.

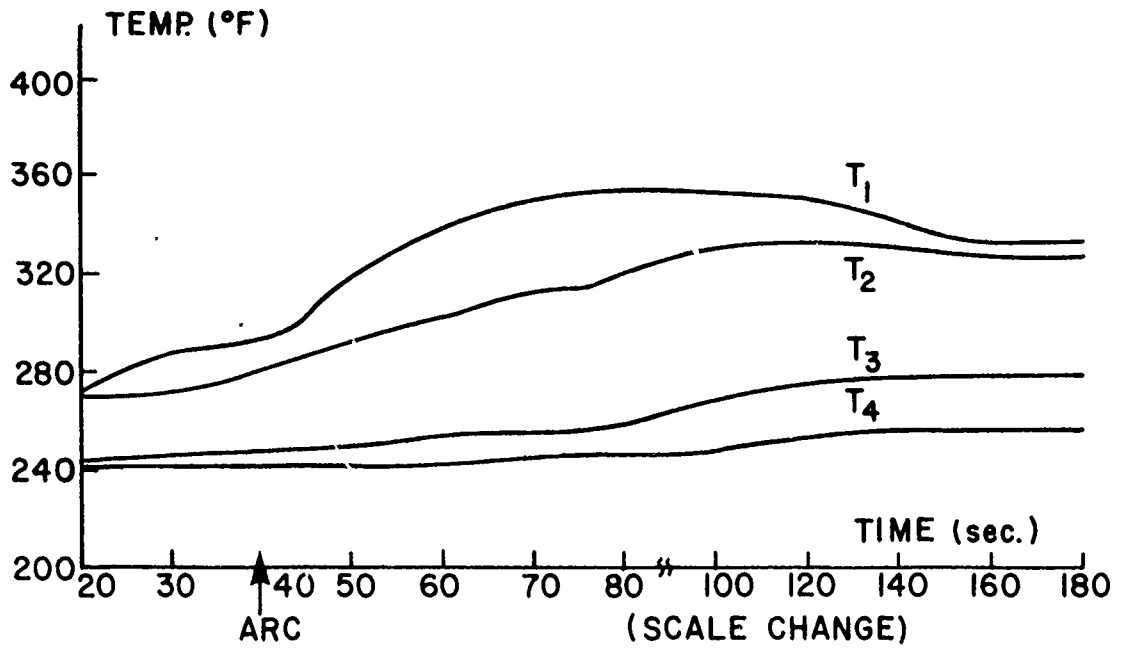


FIGURE 2.38 Test plate temperature distribution during Weld Pass 1.

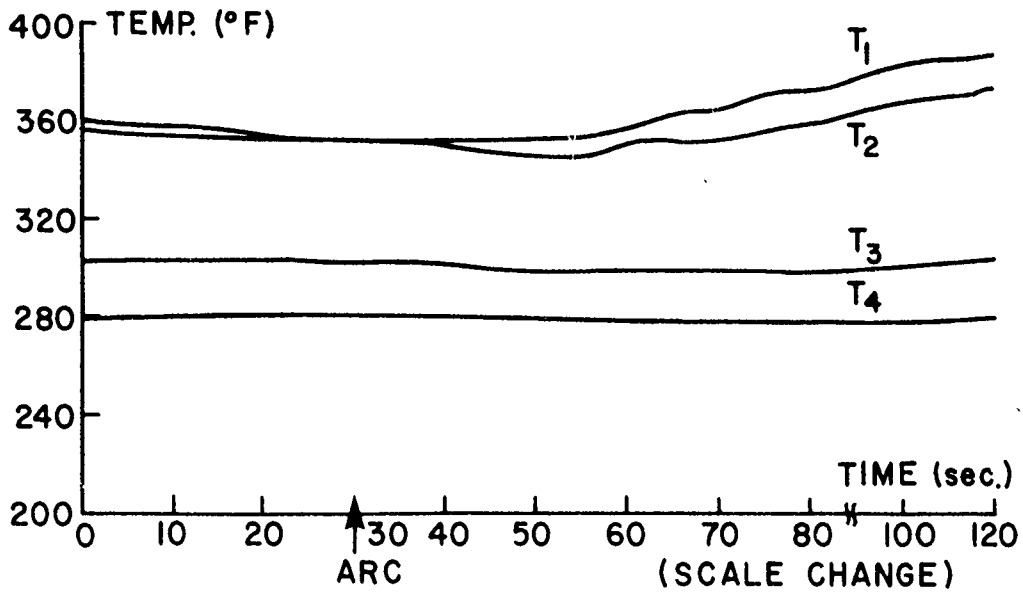


FIGURE 2.39 Test plate temperature distribution during Weld Pass 17.

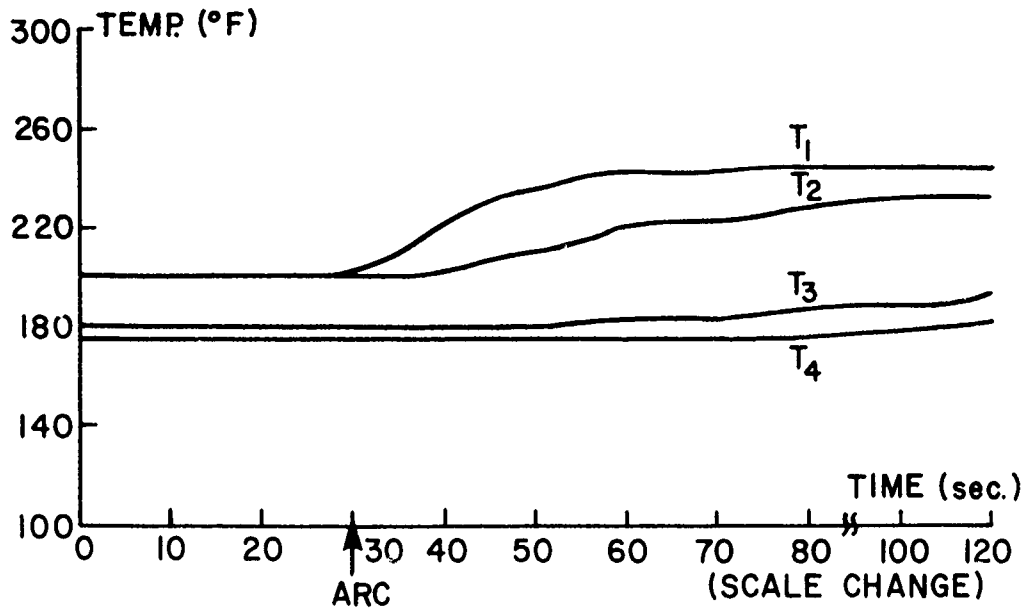


FIGURE 2.40 Test plate temperature distribution during Weld Pass 18.

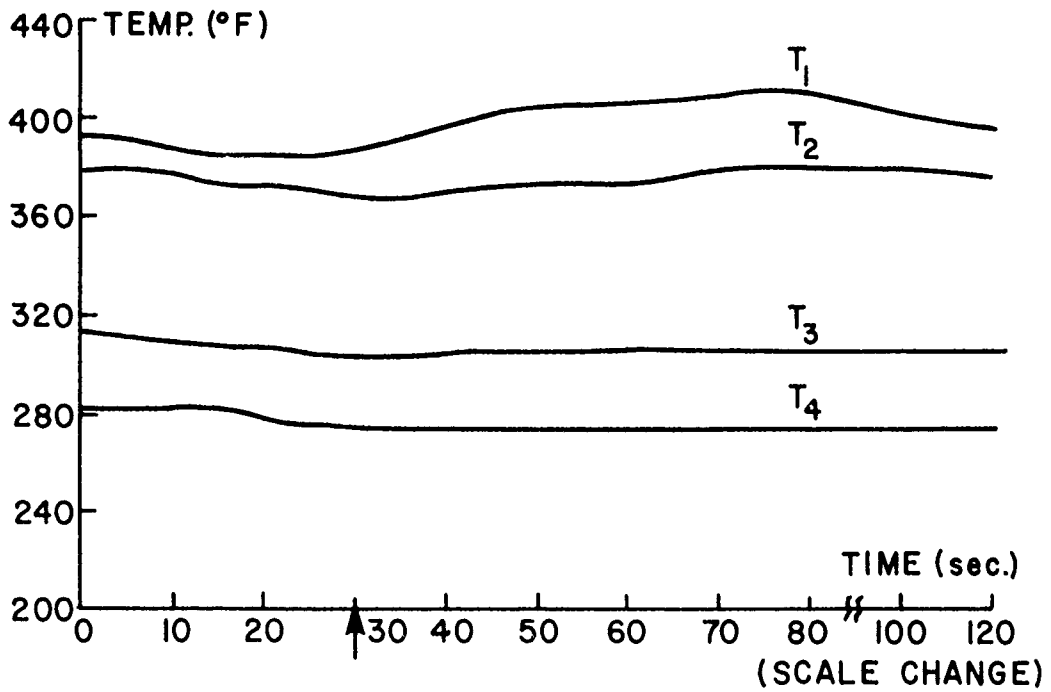


FIGURE 2.41 Test plate temperature distribution during Weld Pass 36.

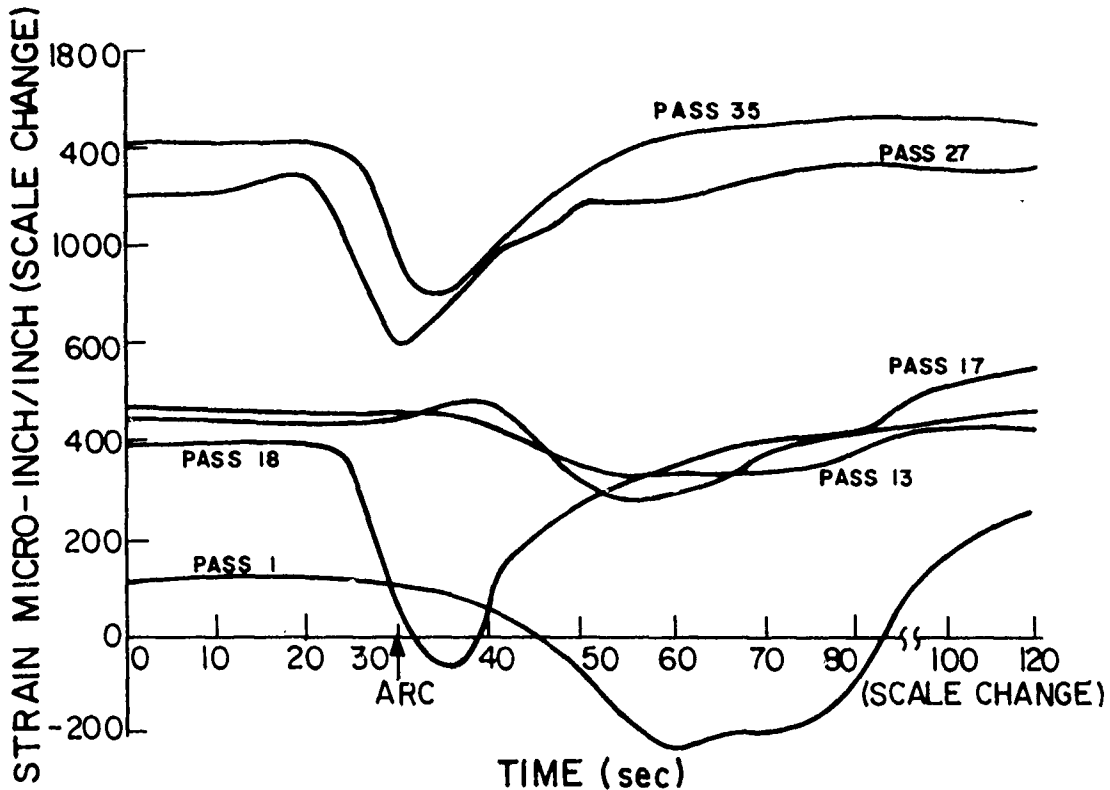


FIGURE 2.42 Comparisons of transverse transient strain distribution for selected weld passes. (1 in. away from weld line)

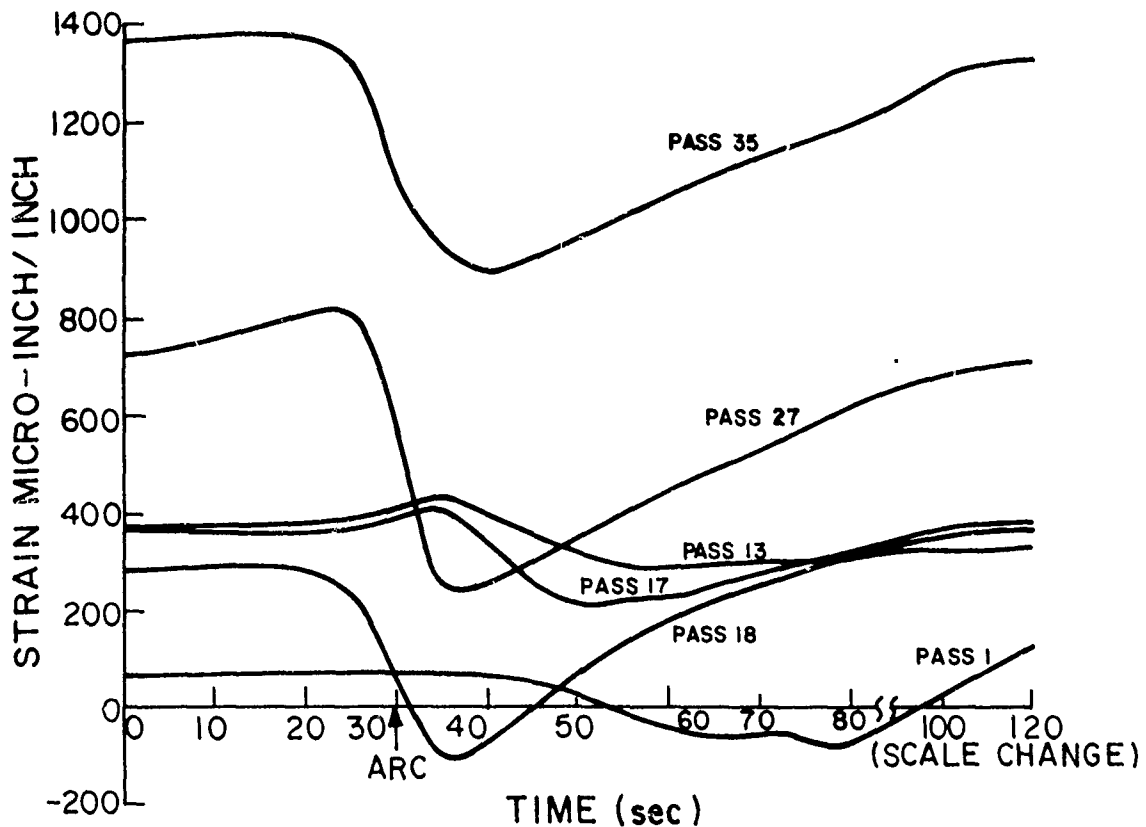


FIGURE 2.43 Comparisons of transverse transient strain distribution for selected weld passes. (1 1/2 in. away from weld line)

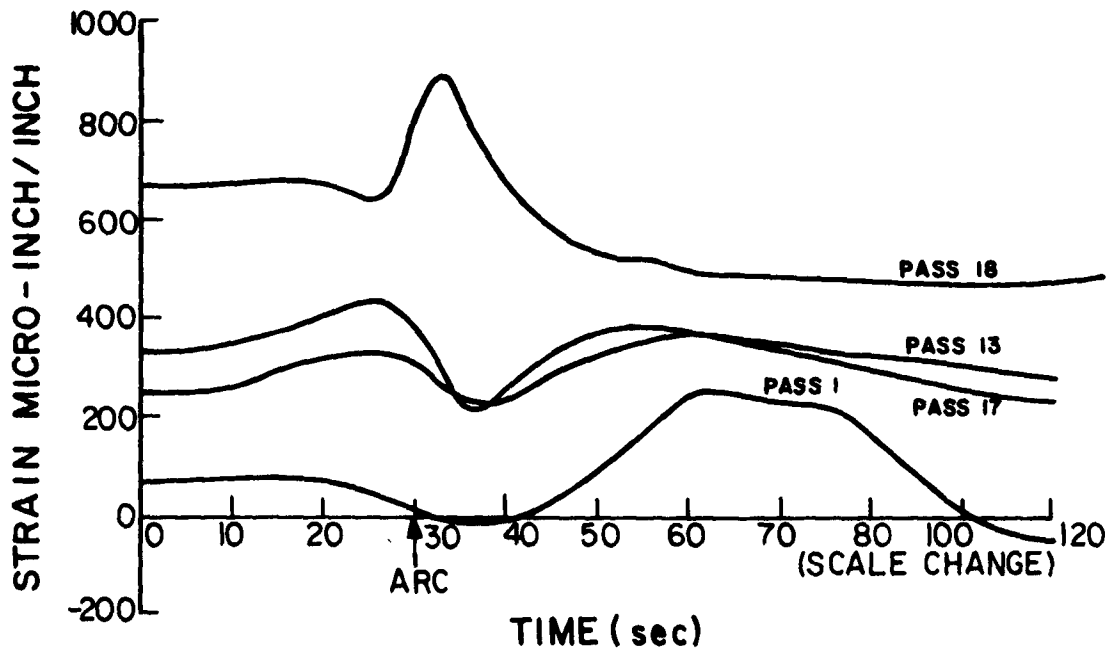


FIGURE 2.44 Comparisons of longitudinal transient strain distribution for selected weld passes. (1 in. away from weld line)

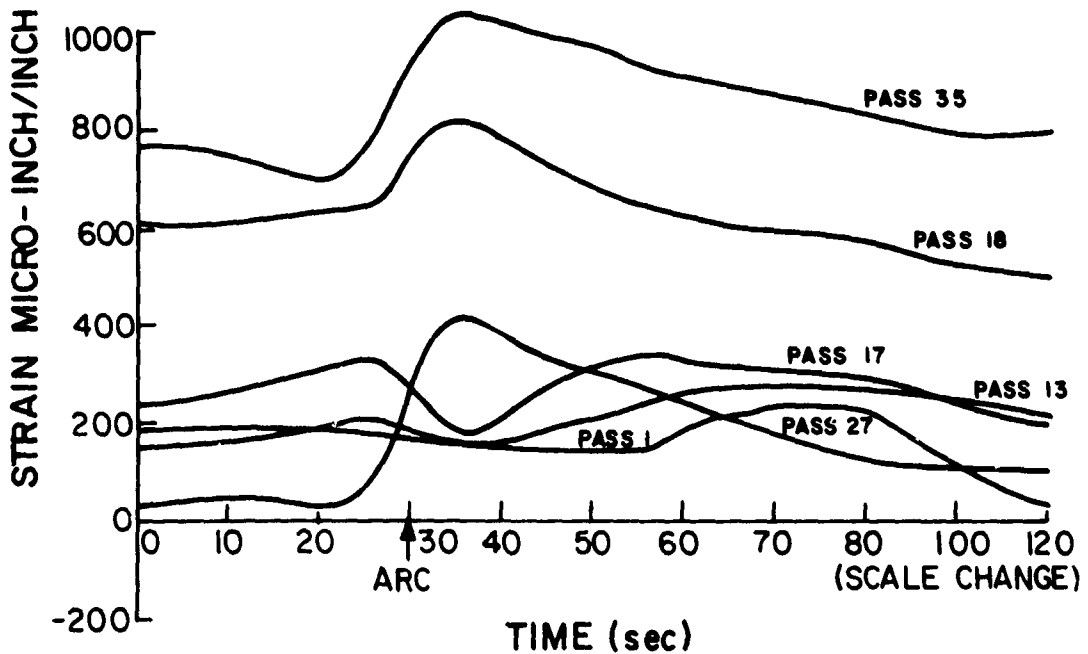


FIGURE 2.45 Comparisons of longitudinal transient strain distribution for selected weld passes. (1 1/2 in. away from weld line)

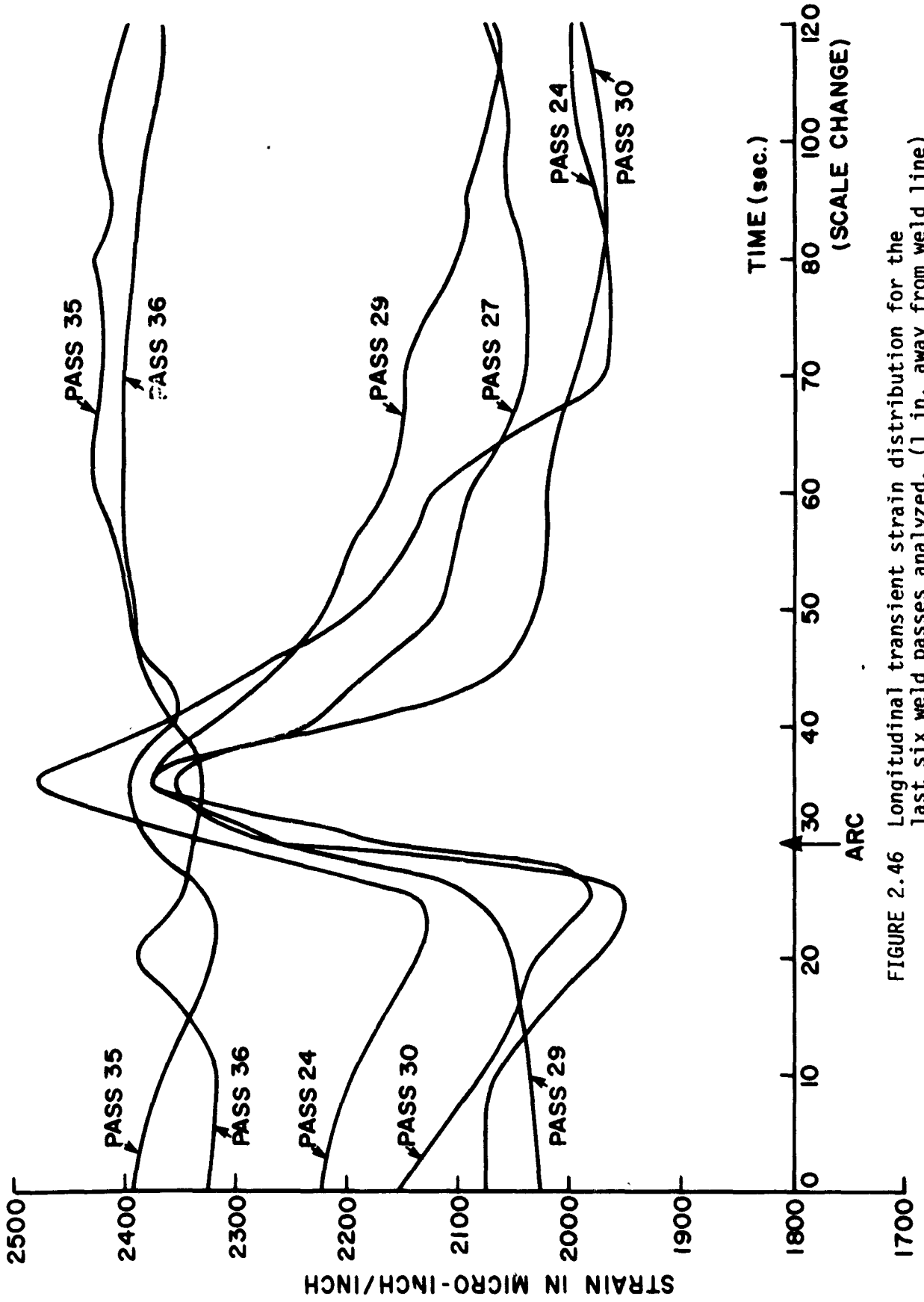


FIGURE 2.46 Longitudinal transient strain distribution for the last six weld passes analyzed. (1 in. away from weld line)

Figure 2.47 shows the COD as a function of one half the crack width, c , and the crack depth, a . Based on these measurements, the stress intensity factor can be calculated based on the linear elastic fracture mechanics theory. These calculations are currently being made by Goncalves as part of his Doctoral dissertation; possible modifications of the theory will be made, if required, to take into account the bluntness of the crack tip and the plastic tip zone.

The above calculations will be compared with a linear elastic finite element analysis that has been developed and which gives the stress intensity factor directly using a special element.

As seen from the above discussion, then, the proposed procedure will directly give the stress intensity factor instead of going through the intermediate step of calculating the strain energy release rate. Nevertheless, this rate can be calculated using the fracture mechanics theory and the results of the aforementioned experiment.

2.7 Analysis of Data (Steps 1.7 and 1.11)

Following is a summary of the analytical work completed during the third year of this research program. A complete description of the analytical and numerical methods used, the obtained results, and comparisons with experimental data will be found in the Doctoral dissertations of V.J. Papazoglou and E. Goncalves, to be published early in 1981.

2.7.1 Joint Degree of Constraint

For the constrained butt joint shown in Figure 2.48 the Joint Degree of Constraint, a kind of spring constant of the structure, is defined by:

$$K_s = \frac{\sigma_o}{\delta}$$

where

σ_o = tensile stress uniformly distributed along the joint

δ = joint transverse displacement (for complex joints an average value is used).

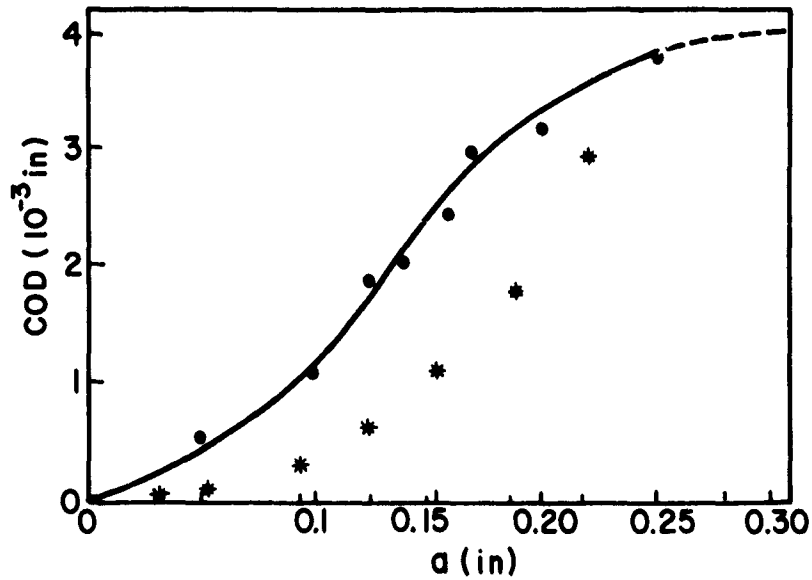
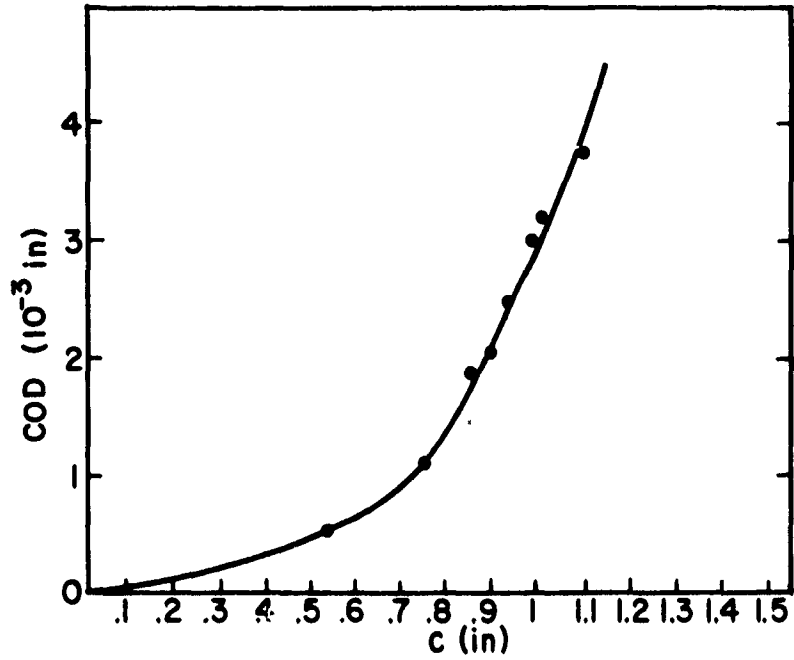


FIGURE 2.47 Crack opening displacement as a function of crack length, $2c$, and crack depth, a .

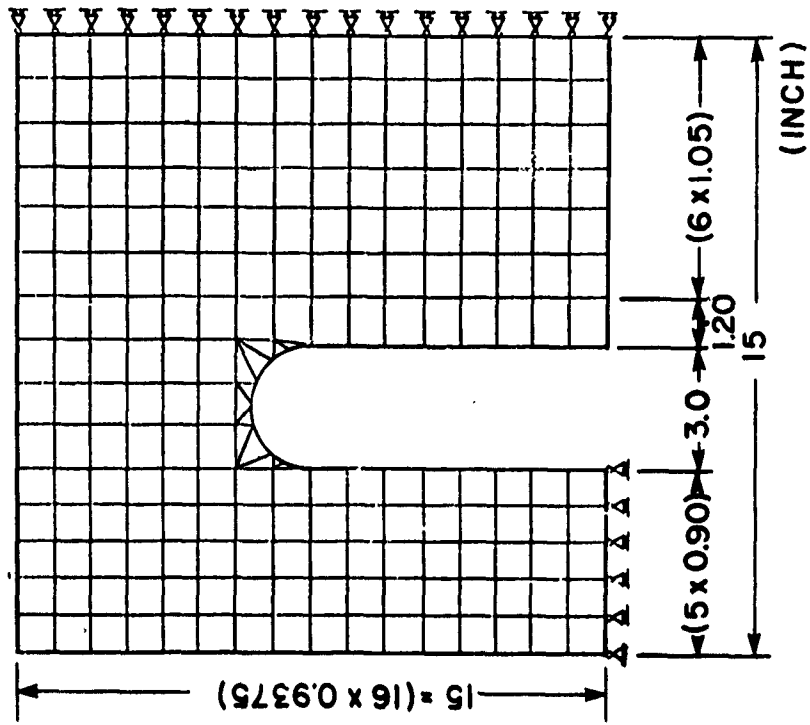


FIGURE 2.49 Finite element mesh of specimen with $B = 18''$.

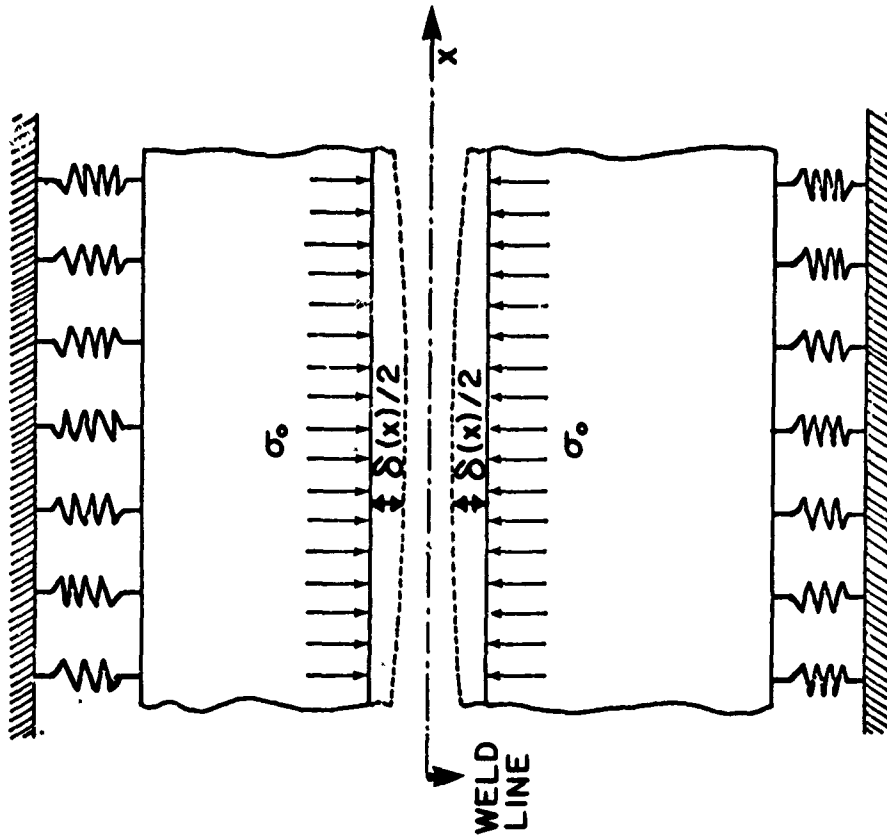


FIGURE 2.48 Schematic representation of a constrained joint.

Using the subroutines of FEABL, a finite element library developed in the Department of Aeronautics and Astronautics at M.I.T., a computer program was developed to calculate the degrees of constraint for the specimens described in Section 2.4 (see Figure 2.23 and Table 2.2). The finite element mesh used is shown in Figure 2.49, for the B = 18" specimens, where it can be noted that quadrilateral and triangular elements were utilized.

Figure 2.50 presents the computed values of the joint degree of constraint for the nine specimens. Figure 2.51 shows that a good correlation exists between the maximum and minimum values of experimentally obtained transient strains in the y-direction and the Degree of Constraint for the HY-130 specimens. Similar results were noted for the SAE 1020 specimens as well as when longitudinal instead of transverse transient strains were used.

2.7.2 Heat Transfer Analysis

Efforts to improve the prediction capabilities of both analytical and numerical solutions of the heat transfer problem during welding have continued throughout the third year of this research program, primarily by Papazoglou. These efforts are summarized below:

Analytical Solutions. The closed-form finite heat source solution - developed during the first two years of this research program and referred to in Section 2.8.1 of the first technical progress report of O.N.R. dated November 30, 1979 - has been modified to take into account the fact that the preheating and/or interpass temperature can be different from the ambient (room) temperature. This modification has resulted in better correlation between experiment and analysis. These correlations, as well as the detailed derivation of the final expressions will be included in Papazoglou's Doctoral dissertation.

Numerical Solutions. Work has continued for improving the multi-purpose finite element computer program ADINAT in order to better predict temperature distributions during welding. ADINAT is capable of performing

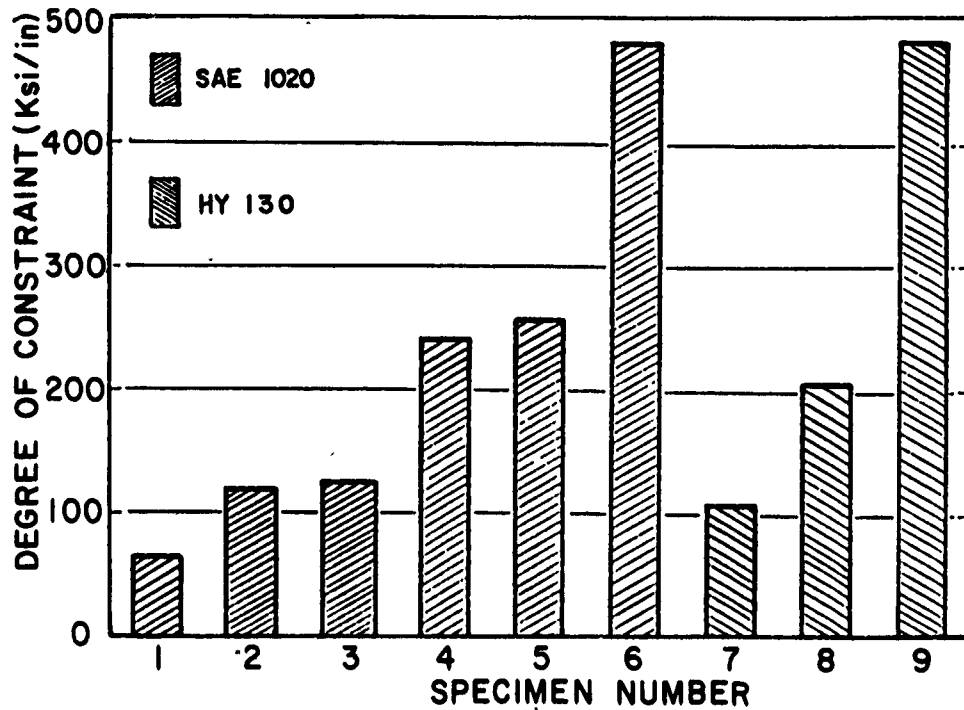


FIGURE 2.50 Computed values of degree of constraint for different specimens.

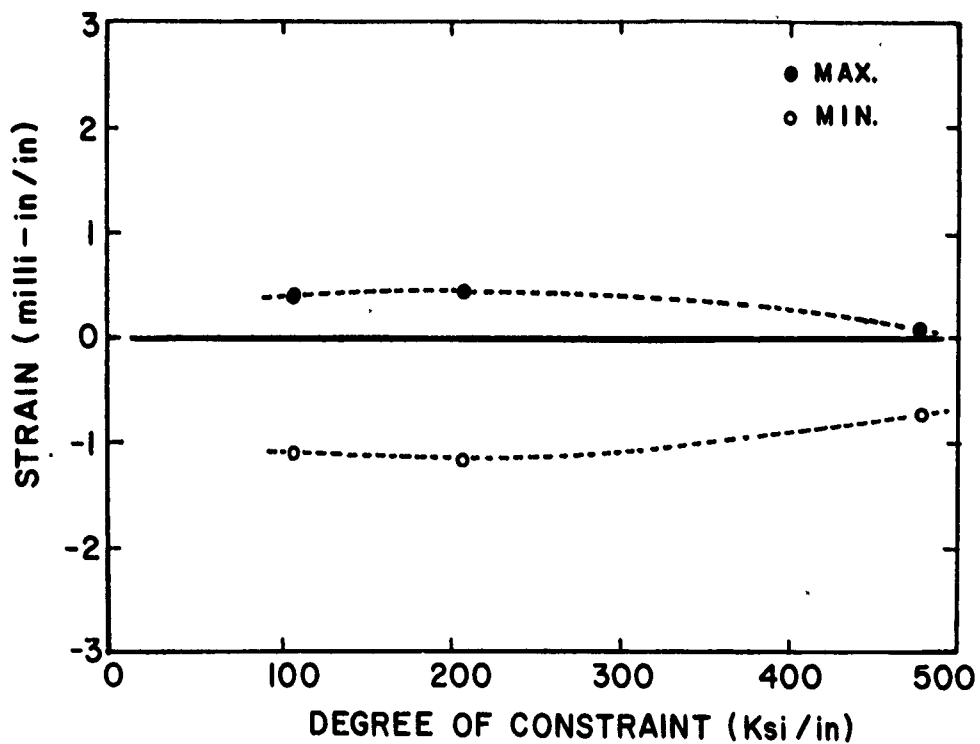


FIGURE 2.51 Maximum and minimum transient strains in y-direction vs. degree of constraint - HY 130.

non-linear heat transfer analyses; the possible non-linearities include temperature dependence of material thermal properties, element birth-and-death options, temperature dependence of convective heat transfer coefficient, and incorporation of radiation heat losses.

The major modification performed was the incorporation of phase transformation effects⁶, which consists of taking into account the latent heat not only during the solid-liquid transformation (melting and solidification) but also during solid-solid (allotropic) transformations.

The program with its modifications was used for modeling the GMA butt welding of 1 in. thick HY-130 plates described in Section 2.3.1 of the Technical Progress Report to O.N.R. dated November 30, 1979. A transverse cross section, 1" thick, located at the mid-portion of the plate was analyzed. Figure 2.52 shows the finite element mesh used. Note that a rather crude mesh was used, and that only the first three passes were analyzed, given the fact that the computer analysis is rather expensive. Nevertheless it was expected that the obtained results would be of a more or less satisfactory nature, as it did happen to be.

At this point some emphasis should be given on the difficulties encountered on establishing reasonable values for the temperature dependent thermophysical properties of HY-130. To the best of our knowledge no tests have been carried out to adequately describe these properties for temperatures beyond 1,000°F. We were therefore forced to use approximations based on the properties of similar materials. These approximations, however, may not be very accurate given the fact that no commercially available steel has chemical composition, especially as far as the combination of carbon and nickel is concerned, close to HY-130. On top of that comes the fact that the commercially available publications specify the Ac_1 and Ac_3 temperatures as being 1210° and 1415°F respectively, whereas plots of the physical properties indicate abrupt changes

⁶Most of this work was actually carried out by Professor Bathe's assistants for proprietary reasons.

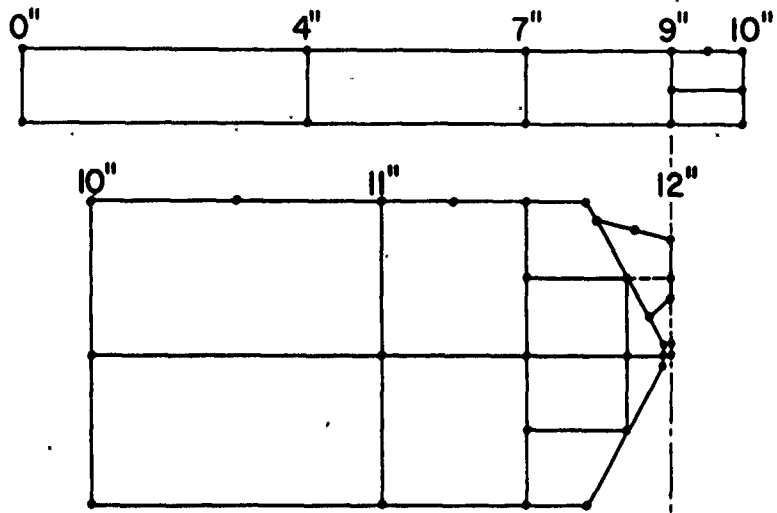


FIGURE 2.52 Finite element mesh for heat transfer analysis (only half of mesh shown).

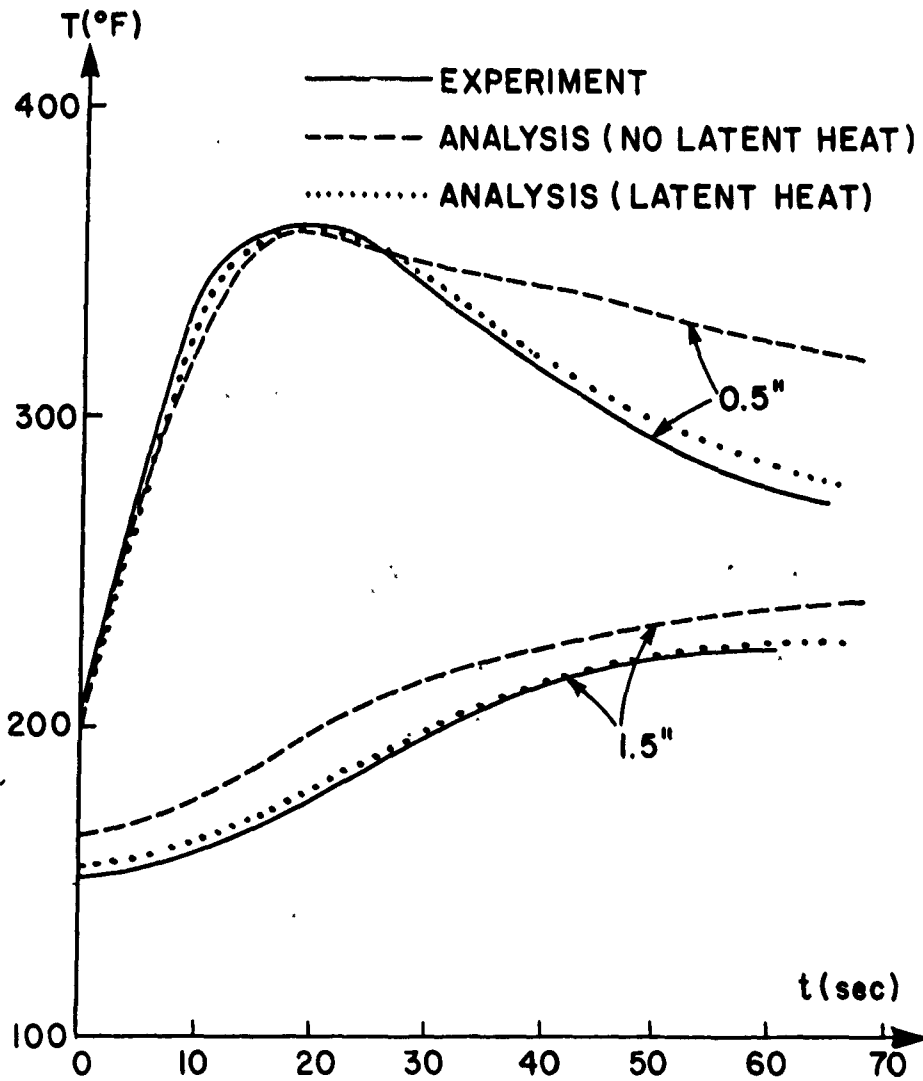


FIGURE 2.53 Temperature distribution during GMA welding of 1" thick HY-130 plate (pass #2).

in their values in the 1400° to 1720°F temperature range.

Figure 2.53 is a sample of the results obtained and their comparison with experiments. Also shown are results obtained by the computer simulation without taking the latent heat effect into consideration. As can be seen, the correlation is much better when the latent heat effect is taken into account.

2.7.3 Stress Analysis

Regarding the stress analysis, efforts have continued for improving the multi-purpose finite element program ADINA in order to make it more suitable in handling the welding problem. It should be noted that ADINA is capable of performing thermo-elastic-plastic and creep analysis of structures in the plane strain, plane stress, and axisymmetric modes by using the classical isothermal constitutive equations as modified for high temperatures. The highly efficient isoparametric formulation is used for the finite element discretization. A so-called birth-and-death option is also available, a fact that enables the modelling of the various welding passes. Finally, ADINA is an overlaid program so that the high speed capability is manifold improved.

At the present time Papazoglou is in the final stages of testing for accuracy the various modifications he implemented on a version of ADINA furnished by Prof. K. J. Bathe of the Department of Mechanical Engineering, M.I.T. The furnished version has as an additional option the printing of strain histories in addition to the stress histories. The addition of this option was necessary since during the welding experiments the measured quantity is strain; it is thus now possible to compare experimental and analytical data.

The major modification involves the incorporation of phase transformation effects, something that plays an important role in the development of residual stresses in high strength quenched and tempered steels. The first step towards this end involves the prediction of the microstructure history in the weld metal and heat affected zone (HAZ). Ideally this step

should have been based on the temperature history obtained from the heat transfer analysis and the rate equations describing the transformation kinetics. Such an approach could not be utilized in the case of HY-130 steel, however, because of lack of appropriate rate equations. The next best way would have been one utilizing the continuous cooling transformation diagrams for HY-130. Although a number of such diagrams became available to us through the DTNSRDC, they did not cover all possible cooling behaviors. As a consequence, they were only used as test cases of the approach actually utilized.

This approach was based on a paper by Grange and Kiefer⁷ who proposed a method for approximately obtaining continuous cooling transformation diagrams using the TTT diagram and invoking the "additivity" principle. Given the availability of the TTT diagram for HY-130, the method was used in deriving CCT diagrams and consequently in predicting microstructure histories. It should of course be understood that the obtained results can be regarded only as approximate, i.e. as a rough indication of what actually happens. Nevertheless, the approximation is thought to be adequate for the purpose of calculating the effect of phase transformation on transient strains and residual stresses.

These phase transformation effects are calculated, using dilatational data and the microstructure history results, as a transformation strain history which is added to the other strain components (namely elastic, plastic, and thermal) to produce the total strain history from which the residual stresses can be calculated.

⁷Grange, R. A., and Kiefer, J. M., "Transformation of Austenite on Continuous Cooling and its Relation to Transformation at Constant Temperature", ASM Transactions, 29(3), 1941, pp. 85-115.

3. PROGRESS OF TASK 2 - CYLINDRICAL SHELLS

December 1, 1979 to November 30, 1980

3.1 General Status

According to the original proposal, the research during the third year of this project would include the following under Task 2:

2.8 Develop details of research plan

2.9 - - - -

2.10 Measurement of residual stresses in specimens made in 2.6⁸

2.11 Analysis of data obtained in 2.10.

This phase of the research program has been in its most part completed as originally planned.

3.2 Development of Details of the Research Plan (Step 2.8).

According to the research plan, the next step under Task 2 would be the measurement of residual stresses developed during the butt welding of the unstiffened cylindrical shells made during the second year. This effort has been completed. Details of the procedure used and the results obtained will be discussed in the next section.

The last step proposed was the analysis of the results obtained. Such analysis has not been performed using the finite element developments discussed in the previous chapter for the same reasons as the ones outlined for the case of butt welds. It is hoped that such an effort can be undertaken during the one-year extension of the current research program.

3.3 Measurement of Residual Stresses in Specimen Made in 2.6(Step 2.10).

3.3.1 Experimental Procedure

Residual stresses were measured on the outside surface of the butt

⁸Step 2.6 states: "Experiment on butt welds between unstiffened cylindrical shells".

welded cylindrical shell which measured 40 in. long, 18 in. O.D., 3/4 in. thick and was made of HY-130 steel (see Figure 3.1).

Upon an initial investigation of the welded specimen, a radial mismatching of the order of 0.040 in. was observed, a fact that led to the decision not to machine the weld reinforcement and hence not to install strain gages on the girth weld line. All measurements were thus to be taken at distances away from the weld line. A total of thirty (30) 90° Rosette strain gages were installed to record the strain relaxations in the axial, x, and circumferential, y, directions. They were divided in six groups of five strain gages each. These groups were located 60° apart from each other as measured in the circumferential direction. For easier identification, the starting/finishing point of the girth weld, located on one of the two seam welds, was defined as the 0° point; then, starting at 13°, the groups were located as previously described (see Figure 3.2b). Within each group the five strain gages were installed along the cylinder's axial direction at distances equal to 1/8", 1/4", 5/8", 1" and 2" from the toe of the widest part of the girth weld (see Figure 3.2c).

The instrumented cylinder was then transported to the machine shop of the Metcut Co., because of lack of appropriate machinery at M.I.T. to handle such a large and heavy specimen. Two 15 in. long pieces were first cut, one from each end, from the shell to facilitate easier handling (see Figure 3.2a), followed by the cutting of six 2 in. wide longitudinal strips each carrying one strain gage group. Finally, each strip was machined down to a 3/4 in. width to allow for total strain relaxation.

3.3.2 Residual Stress Distributions

Using the recorded total strain relaxations and based on Hooke's law the hoop and axial residual stresses, σ_y and σ_x , were then calculated. Figures 3.3(a) to 3.3(f) present the axial distributions of σ_y and σ_x at the six azimuthal angles respectively. Note that in all figures 0 refers to the toe of the weld line. Figures 3.4(a) to 3.4(e) sketch the circumferential distributions of σ_y and σ_x at the five distances from the weld line toe.

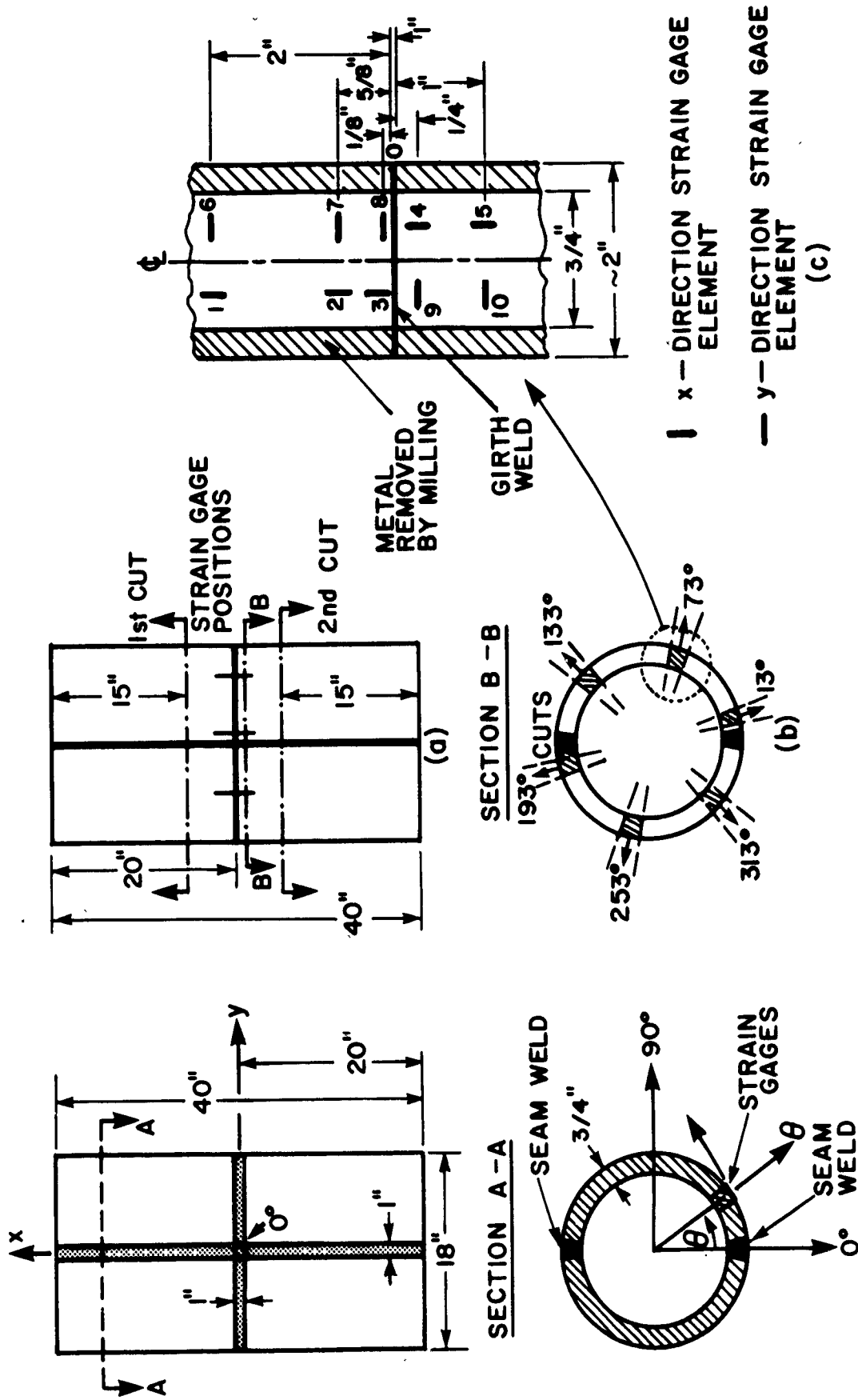


FIGURE 3.1 Dimensions of the welded cylinder under consideration and definition of the coordinates.

FIGURE 3.2 Layout of strain gages, strip positions and illustration of performed cuts.

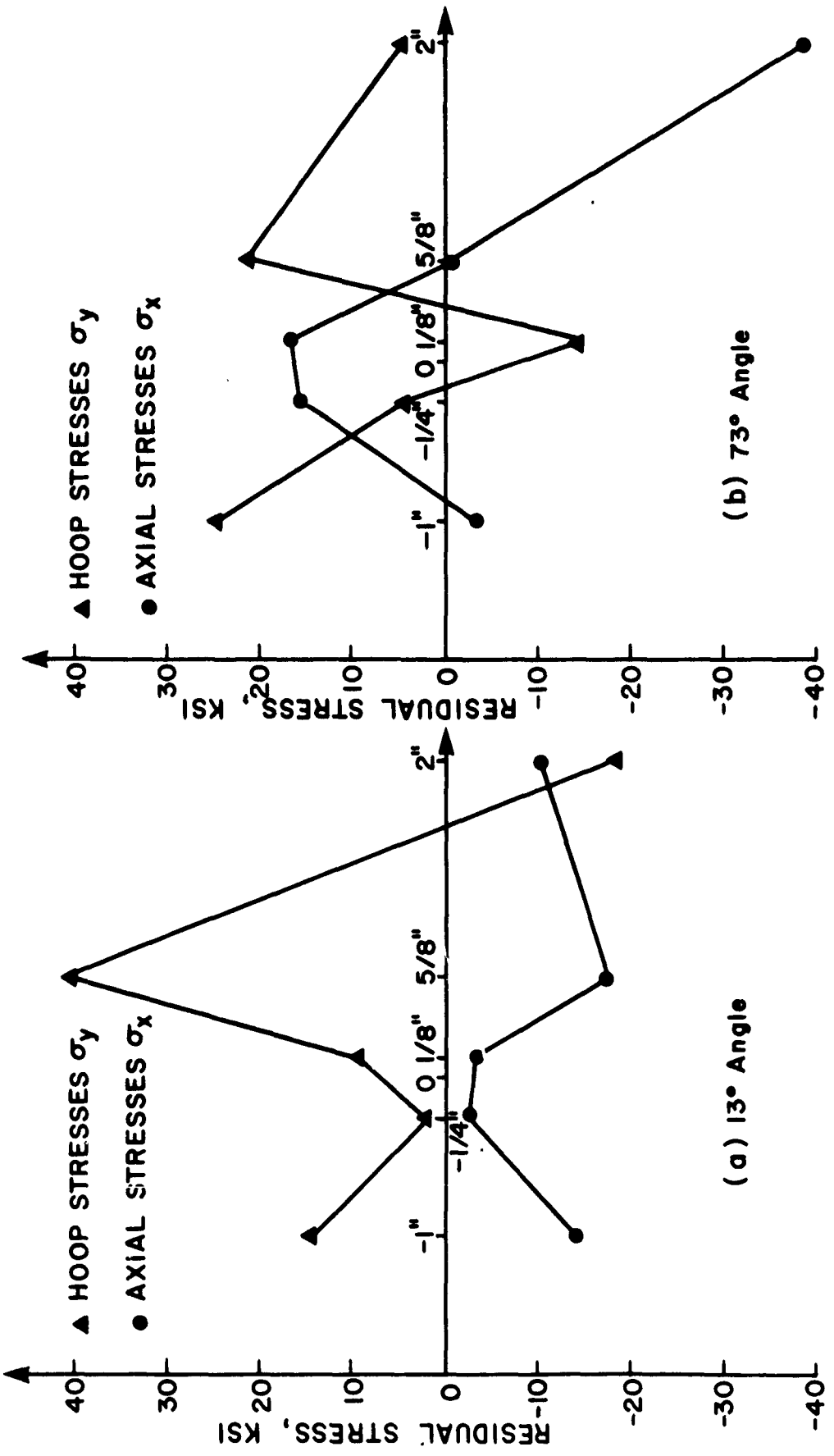


FIGURE 3.3 Axial variation of hoop and axial residual stresses at the six azimuthal angles.
NOTE: Distances measured from toe of weld line.

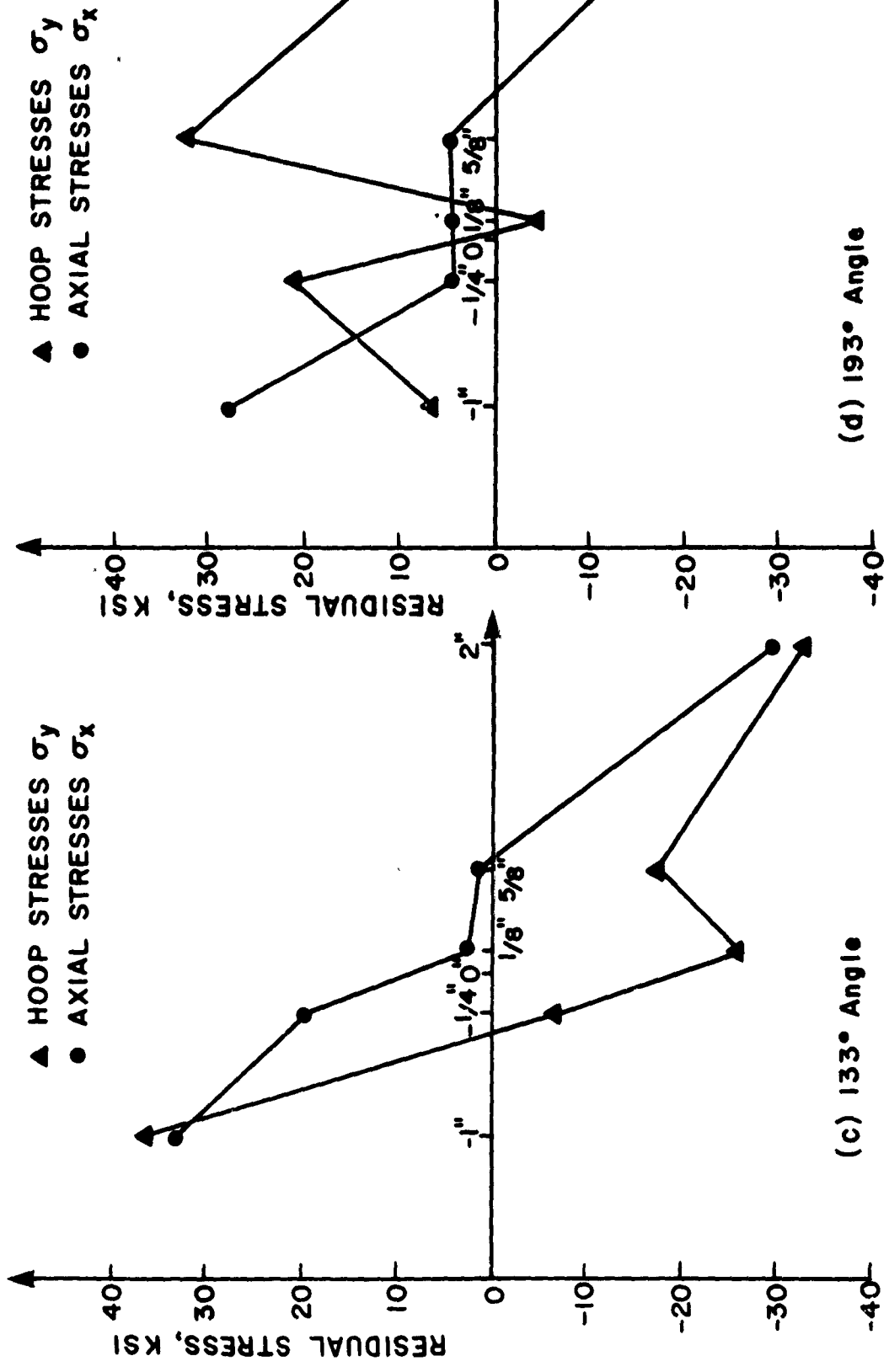
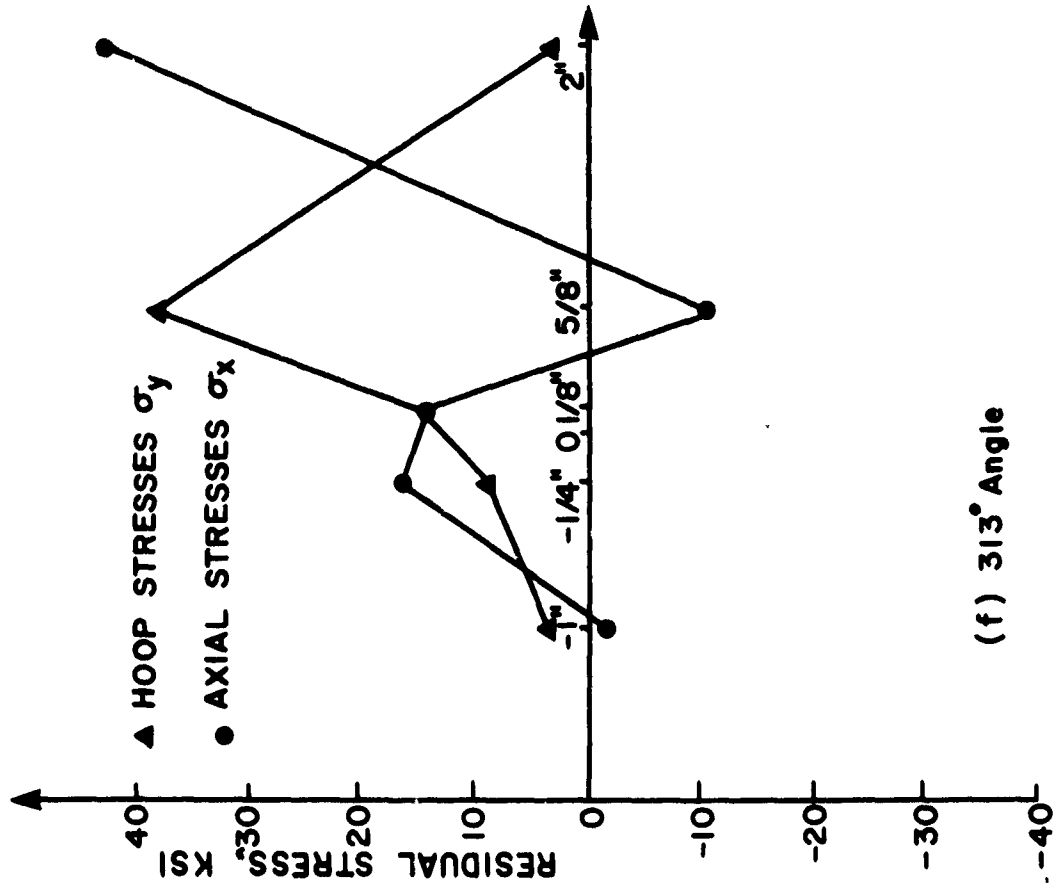
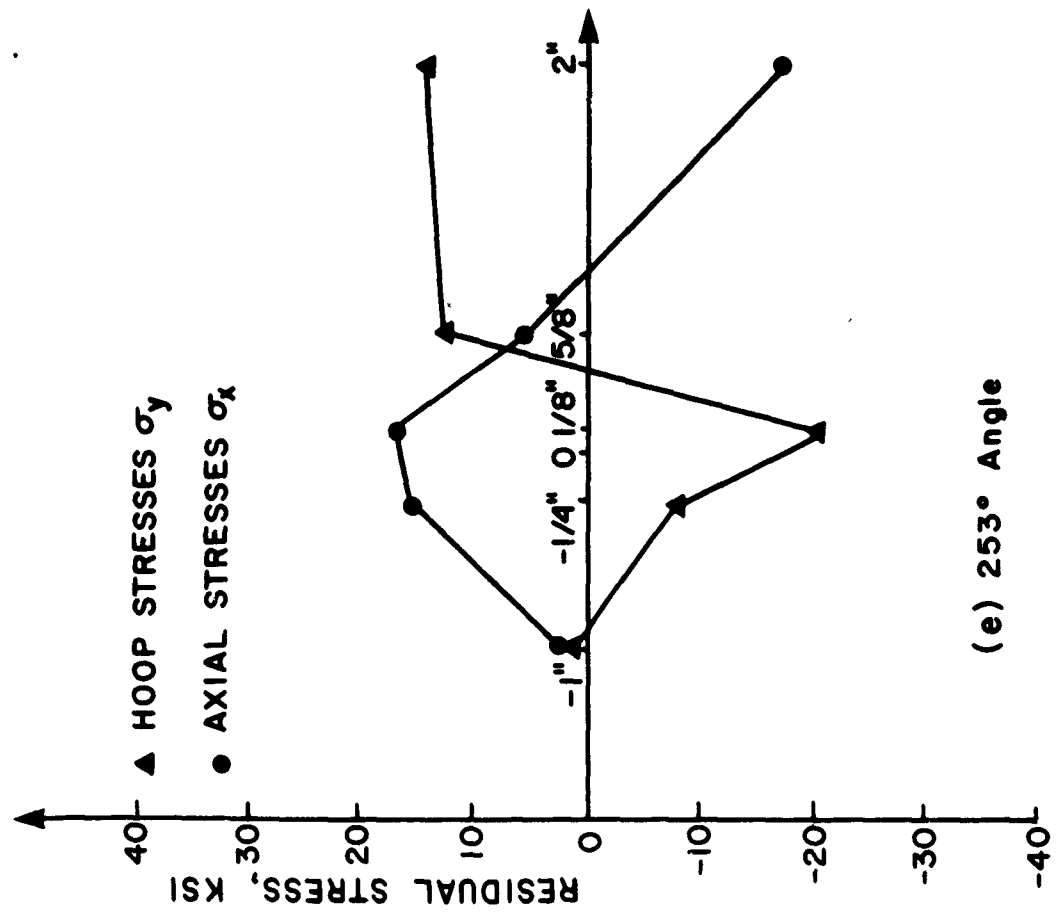


FIGURE 3.3 (cont.)



(f) 313° Angle



(e) 253° Angle

FIGURE 3.3 (cont.)

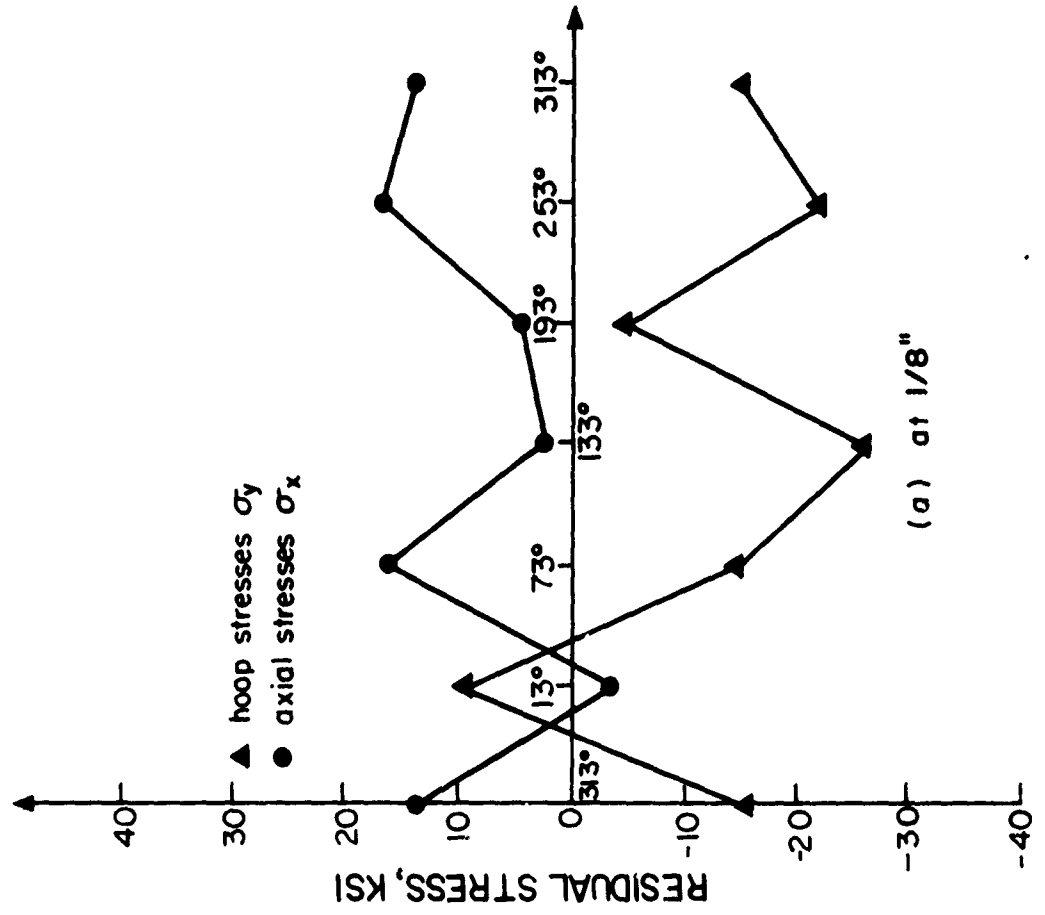
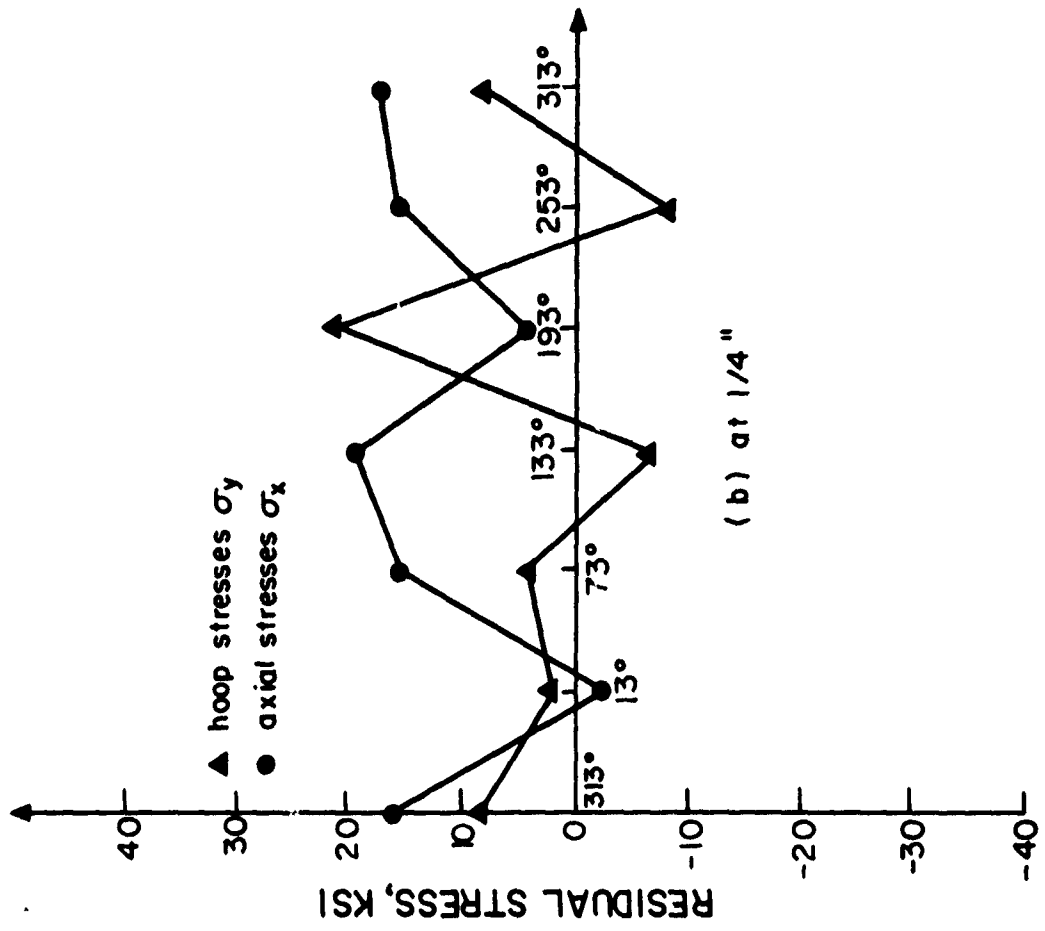
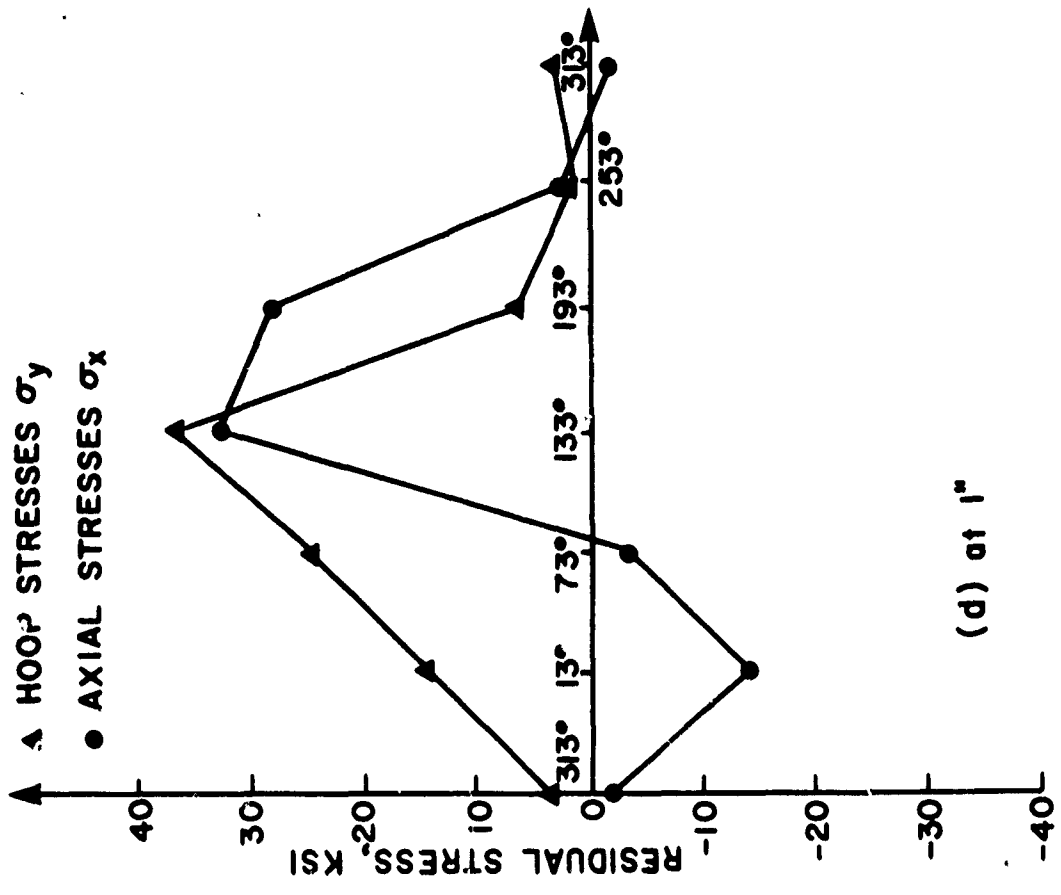
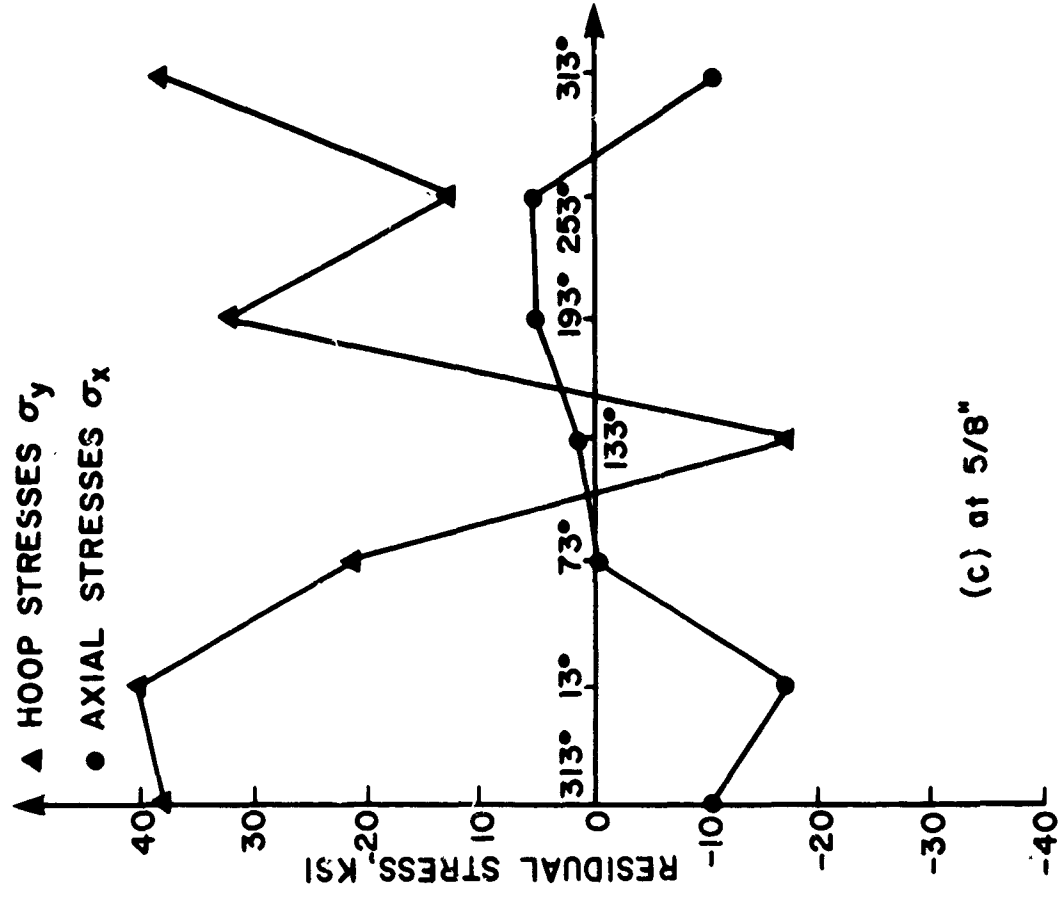


FIGURE 3.4 Circumferential distribution of axial and hoop residual stresses at various distances from toe of girth weld line.



(d) at 1"



(c) at 5/8"

FIGURE 3.4 (cont.)

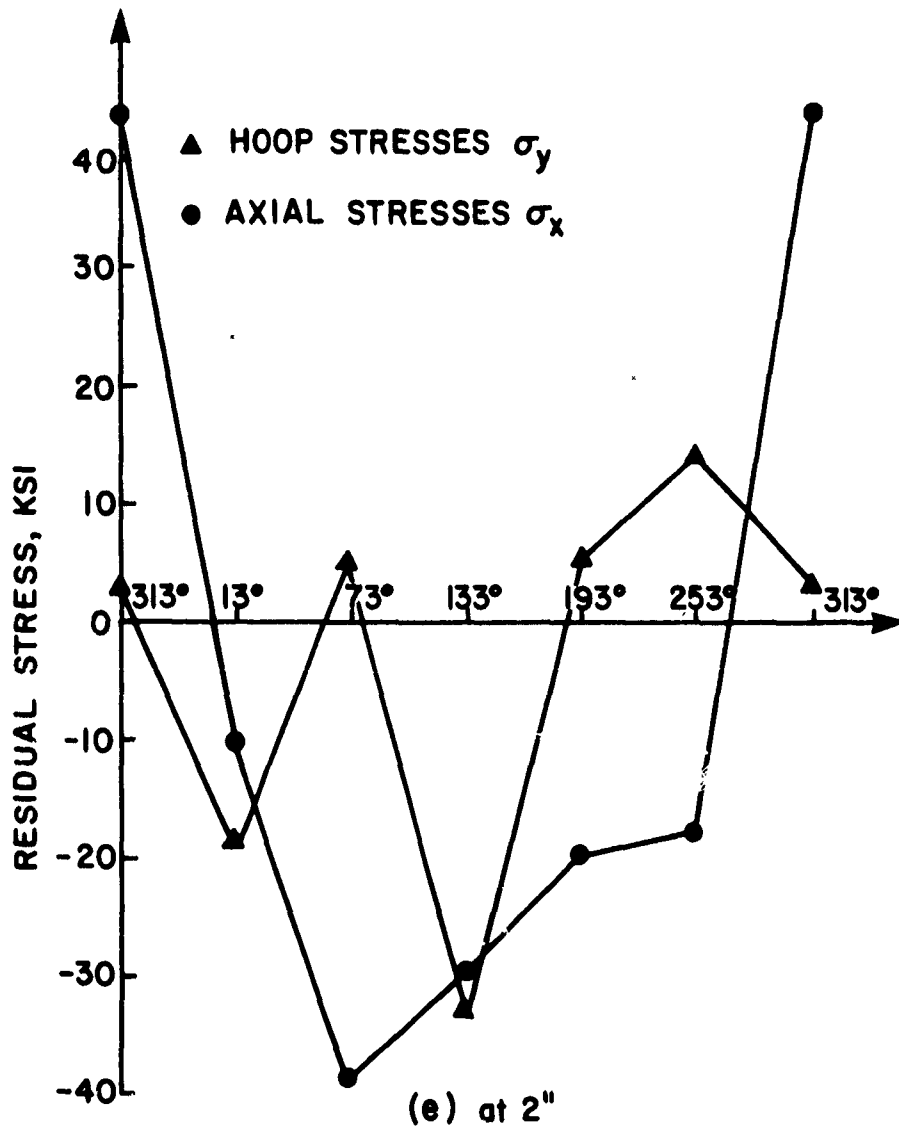


FIGURE 3.4 (cont.)

A close evaluation of the obtained results shows very unusual patterns as compared with those reported by other investigators⁹. First, the "bell shape" observed by others in the axial distribution of residual stresses rarely occurs in the HY-130 specimen. Furthermore, the oscillatory circumferential behavior reported by others does occur in the present specimen as well, but it shows a random rather than a normal pattern. The above lead to the conclusion that the distribution of residual stresses is not axisymmetric, a fact that can be explained not only by the presence of the two seam welds but also by the way they were performed - not simultaneously but each one separately.

Moreover, it is recommended that in any future experiment care should be taken to avoid any mismatching so that strain gages can be installed on the girth weld line. Finally, three-element rosette strain gages should be used in any future investigation to facilitate the calculation of the principal stresses as well.

⁹ Ellingson, W.A., and Shack, W.J., "Residual Stress Measurement on Multipass Weldments of Stainless Steel Piping",

4. PUBLICATIONS AND DEGREES GRANTED

4.1 Publications

Work based on Office of Naval Research sponsored programs has resulted in the following publications during the previous year.

4.1.1 Books

Masubuchi, K., "Analysis of Welded Structures - Residual Stresses, Distortion and Their Consequences", Pergamon Press, Oxford/New York, 1980.

4.1.2 Papers

- Masubuchi, K., "Models of Stresses and Deformation Due to Welding; A Review", Conference on Modeling of Casting and Welding Processes, Franklin Pierce College, Rindge, New Hampshire, August 4-8, 1980.

- Masubuchi, K., and Papazoglou, V.J., "Thermal Strains and Residual Stresses in Heavy HY-130 Butt Welds", 1980 Fall Meeting of SESA, Ft. Lauderdale, Florida, October 12-15, 1980.

- Papazoglou, V.J., and Masubuchi, K., "Analytical Methods for Determining Temperatures, Thermal Strains, and Residual Stresses Due to Welding", 1980 ASM Materials and Processes Congress, Cleveland, Ohio, October 28-30, 1980.

It is expected that several other papers will be published after the completion of the current research program.

4.2 Degrees Granted

The following degrees have been granted to students working on this project¹⁰ during its third year:

Coumis, G.A.: Master of Science in Naval Architecture and Marine Engineering, and Master of Science in Mechanical Engineering.

¹⁰Note that some of these students were U.S. or allied countries' Navy Officers and so their services were furnished at no cost to the project.

Sousa Sa, P.A., Ocean Engineer, and Master of Science in Mechanical Engineering.

Goncalves, E.: Master of Science in Ocean Engineering, and Master of Science in Materials Science.

Suchy, A.F.: Ocean Engineer

4.3 Theses Completed

The following theses, containing information included in this technical progress report, have been completed:

1. Coumis, G.A., "An Experimental Investigation of the Transient Thermal Strain Variation and the Triaxial Residual Stress Field Generated Due to Electron Beam Welding of Thick HY-130 Plates", S.M. Thesis, M.I.T., June 1980.

2. Sousa Sa, P.A., "Investigation of Triaxial Residual Stress Distribution Remaining After GMA Welding of Thick HY-130 Steel Plates", Ocean Engineer Thesis, M.I.T., January 1981.

3. Goncalves, E., "Investigation of Welding Heat Flow and Thermal Strain in Restraint Steel Plates", S.M. Thesis, M.I.T., May 1980.

4. Suchy, A.F., "Investigation of Temperature Distribution and Thermally Induced Thermal Strains in Highly Restrained, Thick, HY-130 Steel Plate Weldments", Ocean Engineer Thesis, M.I.T., June 1980.